Science of the Total Environment 649 (2019) 846–865

Contents lists available at ScienceDirect

Science of the Total Environment

journal homepage: www.elsevier.com/locate/scitotenv

Simulation of regional irrigation requirement with SWAT in different agro-climatic zones driven by observed climate and two reanalysis datasets

Bhumika Uniyal [a,*], Jörg Dietrich [a], Ngoc Quynh Vu [a,d], Madan K. Jha [b], José Luis Arumí [c]

[a] Institute of Hydrology and Water Resources Management, Leibniz University Hannover, Germany
[b] AgFE Department, Indian Institute of Technology Kharagpur, India
[c] Agricultural Engineering, University of Concepción, Chile
[d] Thuyloi University, 175 Tay Son Street, Dong Da, Hanoi, Vietnam

HIGHLIGHTS

- Application of SWAT in four different agro-climatic zones for simulating irrigation water demand was investigated
- MODIS generated ET was evaluated against the SWAT simulated ET
- Irrigation water requirement was evaluated under different scheduling scenarios
- Use of climate reanalysis data (NCEP and ERA-Interim) for agro-hydrological studies in data scarce catchments was evaluated

GRAPHICAL ABSTRACT

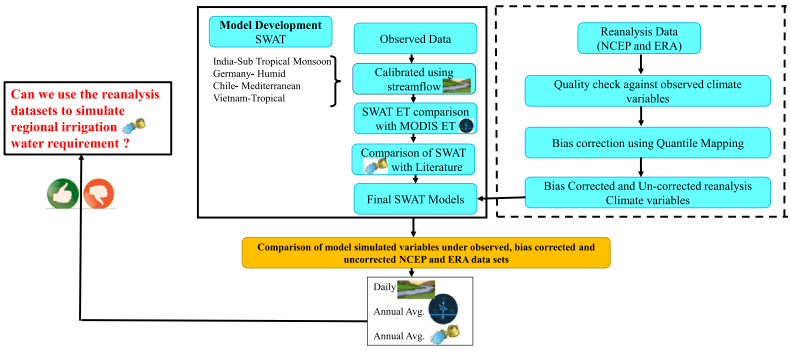

ARTICLE INFO

Article history:
Received 26 April 2018
Received in revised form 7 July 2018
Accepted 19 August 2018
Available online 22 August 2018

Editor: R Ludwig

Keywords:
Irrigation water requirement
SWAT
Auto-irrigation
Agro-climates
MODIS
Reanalysis data

ABSTRACT

Irrigation water is one of the most substantial water uses worldwide. Thus, global simulation studies about water availability and demand typically include irrigation. Nowadays, regional scale is of major interest for water resources management but irrigation lacks attention in many catchment modelling studies. This study evaluated the performance of the agro-hydrological model SWAT (Soil and Water Assessment Tool) for simulating streamflow, evapotranspiration and irrigation in four catchments of different agro-climatic zones at meso-scale (Baitarani/India: Subtropical monsoon; Ilmenau/Germany: Humid; Itata/Chile: Mediterranean; Thubon/Vietnam: Tropical). The models were calibrated well with Kling-Gupta Efficiency (KGE) varying from 0.74–0.89 and percentage bias (PBIAS) from 5.66–6.43%. The simulated irrigation is higher when irrigation is triggered by soil-water deficit compared to plant-water stress. The simulated irrigation scheduling scenarios showed that a significant amount of water can be saved by applying deficit irrigation (25–48%) with a small reduction in annual average crop yield (0–3.3%) in all climatic zones.

Many catchments with a high share of irrigated agriculture are located in developing countries with a low availability of input data. For that reason, the application of uncorrected and bias-corrected National Centers for Environmental Prediction (NCEP) and ERA-interim (ERA) reanalysis data was evaluated for all model scenarios. The simulated streamflow under bias-corrected climate variables is close to the observed streamflow with ERA performing better than NCEP. However, the deviation in simulated irrigation between observed and reanalysis climate varies from −25.5–45.3%, whereas the relative irrigation water savings by deficit irrigation could be shown by all climate input data. The overall variability in simulated irrigation requirement depends mainly on

* Corresponding author.
E-mail address: uniyal@iww.uni-hannover.de (B. Uniyal).

https://doi.org/10.1016/j.scitotenv.2018.08.248

the climate input data. Studies about irrigation requirement in data scarce areas must address this in particular when using reanalysis data.

1. Introduction

The major proportion (about 70%) of the world's water resources is consumed by agriculture although the share of total water use varies drastically under different continents from around 10% in Europe to nearly 90% in South Asia (http://www.fao.org/nr/water/aquastat). However, fast population growth will increase the demand for food, resulting in increased future demand for agricultural irrigation. Rabie et al. (2013) postulated in a global study that 52 countries will face a water deficit crisis by 2025. Irrigated agriculture has expanded by 480% (47.3 to 276.3 Mha) since the last century. Nowadays, 18% of crop land is irrigated and the rest accounts for rainfed agriculture. The increase in irrigated agriculture is majorly concentrated to developing countries as they are more effected by population growth (Rockström and Falkenmark, 2000; Bruinsma, 2003; Siebert et al., 2005; Scanlon et al., 2007).

Water demand and water availability are two main parameters for effective water resources management and water scarcity is a main driver for water resources planning and optimization. In order to overcome the probable future water stress and to ensure food security, the irrigation water use efficiency must be optimized. Crop water requirement is the fundamental input for regional planning and policy making for irrigated agriculture (Santhi et al., 2005). Besides meteorological variables, crop water requirement also depends on soil physical properties and crop parameters like leaf area index, crop stage, rooting depth etc. (Doorenbos and Pruitt, 1977; Allen et al., 1998).

Hydrological models are tools that can simulate dynamic hydrological processes taking into consideration the spatio-temporal distribution of water in different compartments (Zuo et al., 2015). Irrigation requirement is mostly simulated at field scale for operational purpose to optimize the water use at farm scale by using one dimensional soil hydraulic models like SWAP (Soil-Water-Atmosphere-Plant System, van Dam et al., 1997; Droogers and Bastiaanssen, 2002; Singh et al., 2006; Ma et al., 2011) and Daisy (Abrahamsen and Hansen, 2000). However, there has been an increase in the number of studies on optimizing the resource allocation at aggregated scales like command area, catchment or watershed scale (Bastiaanssen et al., 2000). Early models for quantifying the irrigation water requirement at aggregated scale are CADSM (Command Area Decision Support Model, Walker et al., 1995) and EPIC (Erosion Productivity Impact Calculator, Williams et al., 1989; Meinardus et al., 1998). With the advanced application of remote sensing techniques, SEBAL (Surface Energy Balance Algorithm for Land, Bastiaanssen et al., 1998; Zwart and Bastiaanssen, 2007; Teixeira et al., 2009; Allen et al., 2011) was developed. Conceptual hydrological models allow the simulation of larger catchments including horizontal flows of water. Examples with application in irrigated catchments are SLURP (Semi-distributed, Land-Use-based, Runoff Processes, Barr et al., 1997; Kite, 1998; Kite and Droogers, 2000), SWAT (Soil and Water Assessment Tool, Arnold et al., 1998; Neitsch et al., 2011), WaSIM (Water flow and Balance Simulation Model, Niehoff et al., 2002; Schulla and Jasper, 2007) and WEAP (Water Evaluation and Planning System, Danner, 2006; Mehta et al., 2013; Esteve et al., 2015). Moreover, several studies have also been carried out by upscaling field scale models and by nesting the best components of different models (hydrology + plant growth; Ground water + plant growth). Jiang et al. (2015) used SWAP-EPIC for assessing the performance of irrigation and water productivity in the irrigated areas of middle Heihe River, China. Whereas, the irrigation performance was also estimated by using SEBAL and SWAP in Gediz Basin, western Turkey by Droogers and Bastiaanssen (2002).

Nowadays, the interpretation algorithms of satellite imagery from the terra moderate resolution imaging spectroradiometer (MODIS) have been approved (Mu et al., 2013) and used by many researchers in assessing the spatio-temporal hydrologic behavior of agricultural catchments (Stehr et al., 2009; Tang et al., 2009b; Zhang et al., 2009; Emam et al., 2017). Remote sensing can provide satisfactory estimates of irrigated areas and also crop water indicators by capturing the phenological development of crops through multi-temporal image classification (van Niel and McVicar, 2004; Thenkabail et al., 2009; Ozdogan et al., 2010; Pervez and Brown, 2010; Conrad et al., 2011; Romaguera et al., 2012; Peña-Arancibia et al., 2016; Zhang et al., 2018). Errors in the remotely sensed actual evapotranspiration (ET) are generally in the order of 10–20% in Australia (Glenn et al., 2011), whereas, the specific MODIS ET product was reported to have an error of 24.1% relative to the flux towers (Mu et al., 2013; Vervoort et al., 2014). In this paper, we always refer actual evapotranspiration as ET.

Reanalysis data from different spatial and temporal resolution [e.g., National Centers for Environmental Prediction (NCEP, Saha et al., 2010); ERA-interim, Dee et al., 2011; etc.] have been used in simulating the global as well as regional hydrological response of different agricultural catchments. Essou et al. (2016) compared different climate datasets to perform lumped hydrological modelling over 42 catchments in the United States and later on, evaluated the impacts of combining reanalysis and weather data to check the accuracy in discharge simulation over 460 Canadian watersheds (Essou et al., 2017). Wisser et al. (2008) used NECP data to simulate the global irrigation water demand and confirmed that the weather driven variability in global irrigation was <10% but it could be much higher at national scale (±70%). Since some reanalysis data provide time series of >30 years, therefore they have been increasingly used in studying climate trends (Poveda et al., 2006; Wang et al., 2006; Stammerjohn et al., 2008).

Amongst the hydrological models mentioned above, the application of SWAT has gained momentum during last 10–15 years for modelling agricultural catchments (van Griensven et al., 2012). Santhi et al. (2005) improved the capabilities of SWAT by introducing a canal irrigation component into the model for the effective regional planning of an irrigated agricultural catchment in Rio Grande, U.S. Xie and Cui (2011) developed SWAT for simulating paddy fields in the Zhanghe Irrigation District located in China. Dechmi et al. (2012) used SWAT to simulate the intensive agricultural irrigated catchment of the Del Reguero watershed in Spain. Panagopoulos et al. (2014) evaluated the economic effectiveness of different best management practices for reducing the irrigation water abstraction in Pinios, Greece. Maier and Dietrich (2016) compared different irrigation strategies, where different methods of auto-irrigation implemented into SWAT showed considerably different results for a humid catchment in Germany. Marek et al. (2016) investigated the simulation of the leaf area index (LAI) and ET in SWAT and found deficiencies, which may have an impact on the accuracy of simulated plant water uptake. Chen et al. (2018) proposed an improved auto-irrigation function for SWAT based on field studies in Texas (Chen et al., 2017). In addition to this, SWAT was used to find out the best management practices for irrigation considering crop water requirement, productivity, management strategies costs and crop market prices in Crete, Greece (Udias et al., 2018). The updated SWAT+ model will improve the control of auto-irrigation by decision tables (Arnold et al., 2018).

Irrigation water availability is a key driver to determine cropping patterns. Climate change will potentially affect natural hydrological and plant growth processes around the world. Therefore, cropping patterns/amounts should be adjusted/evaluated for this challenge (Wang et al., 2011; Dubey and Sharma, 2018). Consequently, agro-hydrological models should be evaluated regarding their ability and performance to simulate plant growth and hydrology under climate and management constraints.

The objectives of this study are: (i) to investigate the application of SWAT models in different agro-climatic zones of the world (Chile-Mediterranean; Germany-Humid; India-Sub tropical and Vietnam-Tropical) for simulating irrigation water requirement; (ii) to compare plant water requirement using MODIS generated ET and SWAT simulated ET; (iii) to simulate the irrigation water requirement under different irrigation control scenarios; and (iv) to investigate the use of climate reanalysis datasets like NCEP (National Centers for Environmental Prediction) and ERA-Interim for agro-hydrological studies in data scarce catchments.

2. Study area and data

The study area for this study consists of four different agricultural catchments located in different agro-climatic conditions (Fig. 1). The selection of the four catchments was based on different climatic conditions, spatial location, type of crop grown, size and type of catchment area (mainly agricultural catchments of meso-scale) and data availability. The salient information about these catchments, the data used, irrigation techniques used and the sources of irrigation water are summarized in Table 1. A brief description of the four catchments is provided below.

(1) The Upper Baitarani River basin (1776.6 km^2) lies between 21-22.5° N latitude and 85–86° E longitude and is located in Eastern India, Odisha (Fig. 2). The Baitarani River originates from Guptaganga hills (900 m above MSL) in the Keonjhar district of Odisha. The climate of the study area is characterized as subtropical climate with defined winter, summer and monsoon seasons. More than 80% of the annual rainfall (1165 mm) occurs during June to October. The mean monthly maximum temperature is 34 °C experienced in May, whereas the minimum temperature is 11 °C in January. The dominant type of soil in this basin is 'sandy clay loam', which consists of 22% clay, 13% silt and 65% sand and occupies 50% of the river basin. A majority of soils in the basin are light textured red soils, which have low water-holding capacity, low fertility and high erodibility (Verma and Jha, 2015). Forest comprises the major portion of the land cover (~50% of the area) followed by agriculture (42%) and 10% fallow. Surface water conveyed through canals is used for flood irrigation.

(2) The second studied catchment is a sub-catchment of the Ilmenau River, located in the Federal state of Lower Saxony, Northern Germany. It lies between 52-54°N and 9–11°E (Fig. 2). The average annual rainfall is around 720 mm, which is temporally distributed throughout the year. The soils are mostly sandy-loam (75% sand) and medium sand (95% sand), resulting in low water holding capacity and fast infiltration (Uniyal et al., 2017).

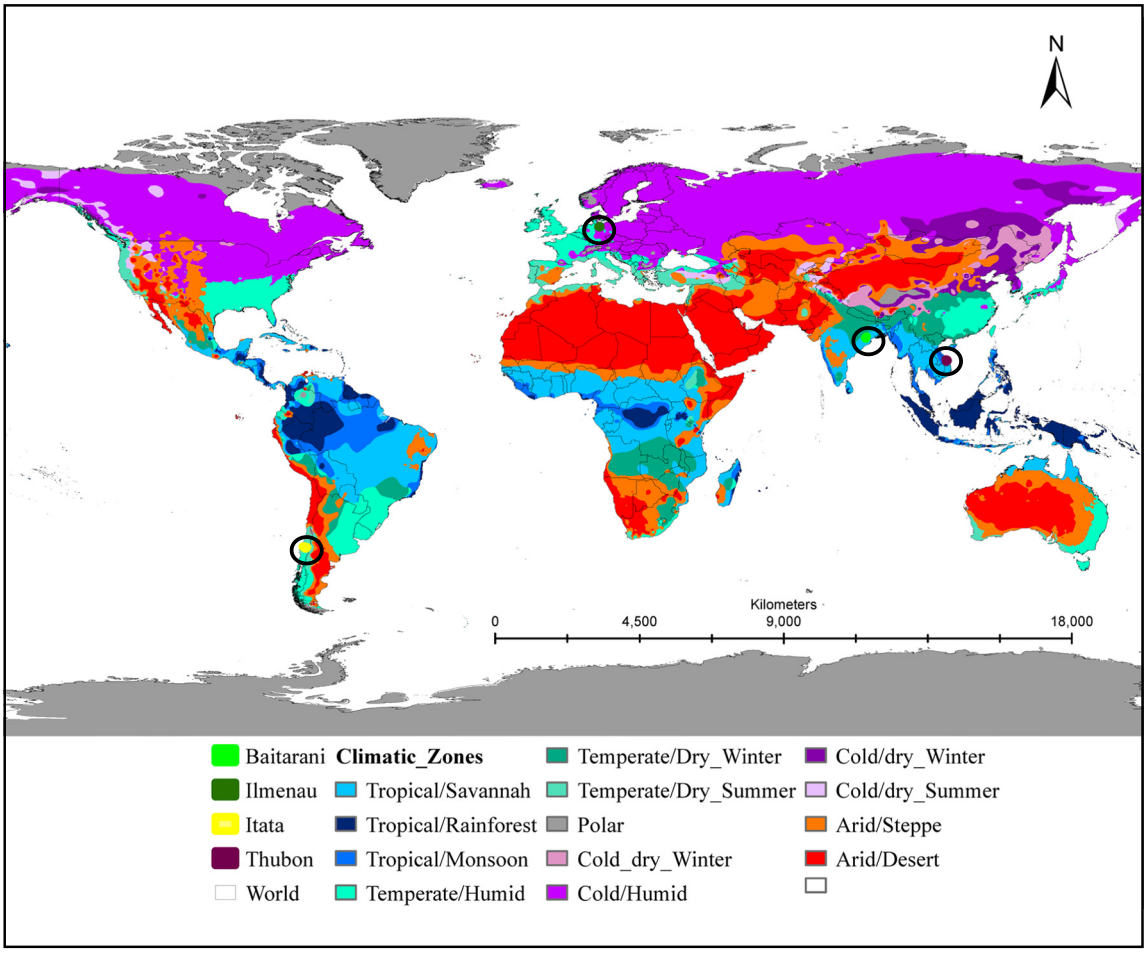

Fig. 1. Location of different catchments around the world with major Köppen-Geiger climatic classification (modified from Peel et al., 2007).

Table 1
General information of the catchments.

Sl. no.	Study area and Köppen-Geiger climatic zones	Area (km^2)	Mean avg. rainfall (mm)	Investigation period	% Agri.-area	Source of irrigation water	Mode/irrigation technique	Dominati-ng crops
1	Baitarani-India (**Aw** -Tropical dry summer) Subtropical-monsoon	1776	1340	1998–2010	42	Canals	Canals Surface irrigation	Rice, pulses, oil seeds
2	Ilmenau-Germany (**Dfb** - Cold warm summer) Humid	1478	720	1979–2010	55	Groundwater	Sprinkler Pressurized Irrigation	Wheat, potato, corn, sugar beet
3	Itata-Chile (**Cfa** - Temperate hot summer) Mediterranean	4529	1420	1979–2010	66	Canals	Canals, drip and sprinkler Pressurized and surface irrigation	Fruit plantations, alfalfa, oats
4	Thubon-Vietnam (**Am** -Tropical monsoon) Tropical	3124	3828	1979–2010	8	Canals	Canals Surface irrigation	Rice

Agricultural land cover is the dominant land use (54%) followed by forest cover (31.5%). Consequently, many fields are irrigated. The irrigation water is mostly extracted from the shallow porous aquifer present in this region and applied via sprinkler systems (Wittenberg, 2003).

(3) The Itata catchment in the Nuble province in Chile is chosen from the Southern Hemisphere for the current research. The Itata catchment is located between 72.4°–71.2°W longitude and 36.4°–37.2°S latitude (Fig. 2). Average annual rainfall of the study area is around 1420 mm, of which >80% occurs in May to October. The mean maximum temperature is 19.4 °C, whereas the mean minimum temperature is 6.9 °C (Muñoz et al., 2016). The major soils in this catchment comprises of mountain alluvium (16.7%) and volcanic soils (11%) with poor soil quality. The major portion of the catchment is comprised of agricultural land use with nearly 48% of the total area followed by the forest land cover (36%). The most popular irrigation techniques followed around this catchment are surface, canal and pressurized irrigation systems and a few center pivot.

(4) The Thubon River originates from the Truong Son mountain range, which is at an altitude of >2000 m above MSL (mean sea level). The catchment is located between the longitudes 107.84°E and 108.47°E, and latitudes 14.95°N and 15.75°N. The catchment has an average annual rainfall of >2000 mm/year. Average maximum temperature is around 26–27 °C in June and July, while average minimum temperature is within 20.5–21.5 °C in December and January. The soils are mostly sandy clay loam covering nearly 83% of the catchment with 26% clay and silt and 48% sand, respectively (Nam et al., 2013). The major land use of the Upper Thubon River catchment (3124 km^2) selected for the study is comprised of 85.38% forest cover followed by 8% agricultural land cover, which is mostly rice grown under rain-fed agriculture (Nay-Htoon et al., 2013).

The selected catchments show huge variability in terms of temporal rainfall distribution ranging from Germany, in which rainfall is distributed throughout the year, to India, which has a clear monsoon season, along with the variation in annual average rainfall amount ranging from 760 mm (Germany) to >2000 mm (Vietnam) [Table. 1(a)]. Therefore, it is worth to explore the performance of the agro-hydrological model (SWAT) for simulating streamflow, evapotranspiration and irrigation water demand under the aforementioned diverse agro-climatic conditions (Table 1).

2.1. Reanalysis data

To assess and manage the water resources available within a river basin, good estimates of hydro-meteorological data, such as precipitation, temperature and streamflow, are required (López et al., 2017). However, many river basins around the world still have a limited number of in-situ observations, being either ungauged (Sivapalan et al., 2003) or poorly gauged (Loukas and Vasiliades, 2014). Several studies have utilized the dynamically downscaled datasets for simulating the hydrology of a watershed (Bastola and Misra, 2013; Polanco et al., 2017). In this study, two datasets from dynamically downscaled climate reanalysis datasets called National Center for Environmental Prediction (0.5°; https://globalweather.tamu.edu/) and ERA-interim (0.125°; http://apps.ecmwf.int/datasets/data/interim-full-daily/levtype=sfc/) were used. Climate Forecast System Reanalysis is a product developed by NCEP, whereas ERA-interim (ERA) daily is a product from European Centre for Medium-Range Weather Forecast. The global models provide daily climate data from 1/1/1979 to 7/31/2014 and 7/31/2017 for NCEP and ERA, respectively.

2.2. Evapotranspiration data

Evapotranspiration acts as a vital link between climate, hydrology and ecology (Gharbia et al., 2018). Long-term direct ground measurements of ET are typically not available and therefore, it is mostly calculated from meteorological variables. Nowadays, remote sensing techniques can be used to calculate spatio-temporal ET indirectly on a larger scale. The precision and accuracy of satellite ET algorithms, which incorporate land surface temperature data are sufficiently high. Therefore, they can be used for enhancing the water management at catchment scale (Cuenca et al., 2013; Steele et al., 2015; Tang et al., 2009a). Moderate Resolution Imaging Spectroradiometer (MODIS) provides valuable spatio-temporal evapotranspiration data which helps to check the evapotranspiration simulated by hydrological models. Spatio-temporal maps of ET were downloaded from 2000 to 2010 using Moderate Resolution Imaging Spectroradiometer (MODIS, Mu et al., 2013, NASA MODIS16A2/A3). It has a spatial resolution of 1 km. MODIS provides cumulative ET for every 8 days interval.

3. Methodology

3.1. Hydrological model setup and calibration

The physically based continuous time scale model, Soil and Water Assessment Tool (SWAT) can simulate water fluxes, plant growth and agricultural land management operations at catchment scale (Arnold et al., 1998). The agro-hydrological SWAT models in this study were developed by using the same model equations and comparable input weather data, crops, etc., for each of the four catchments. This was done to bring the models into comparable level so that model's application in simulating hydrological processes under different agro-climatic conditions can be evaluated. Runoff was simulated by using the SCS curve number method, evapotranspiration was calculated by the Penman-Monteith equation. Furthermore, Muskingum routing was used for routing the flow through the catchment (Neitsch et al., 2011). Vertical processes are performed at hydrological response unit (HRU)

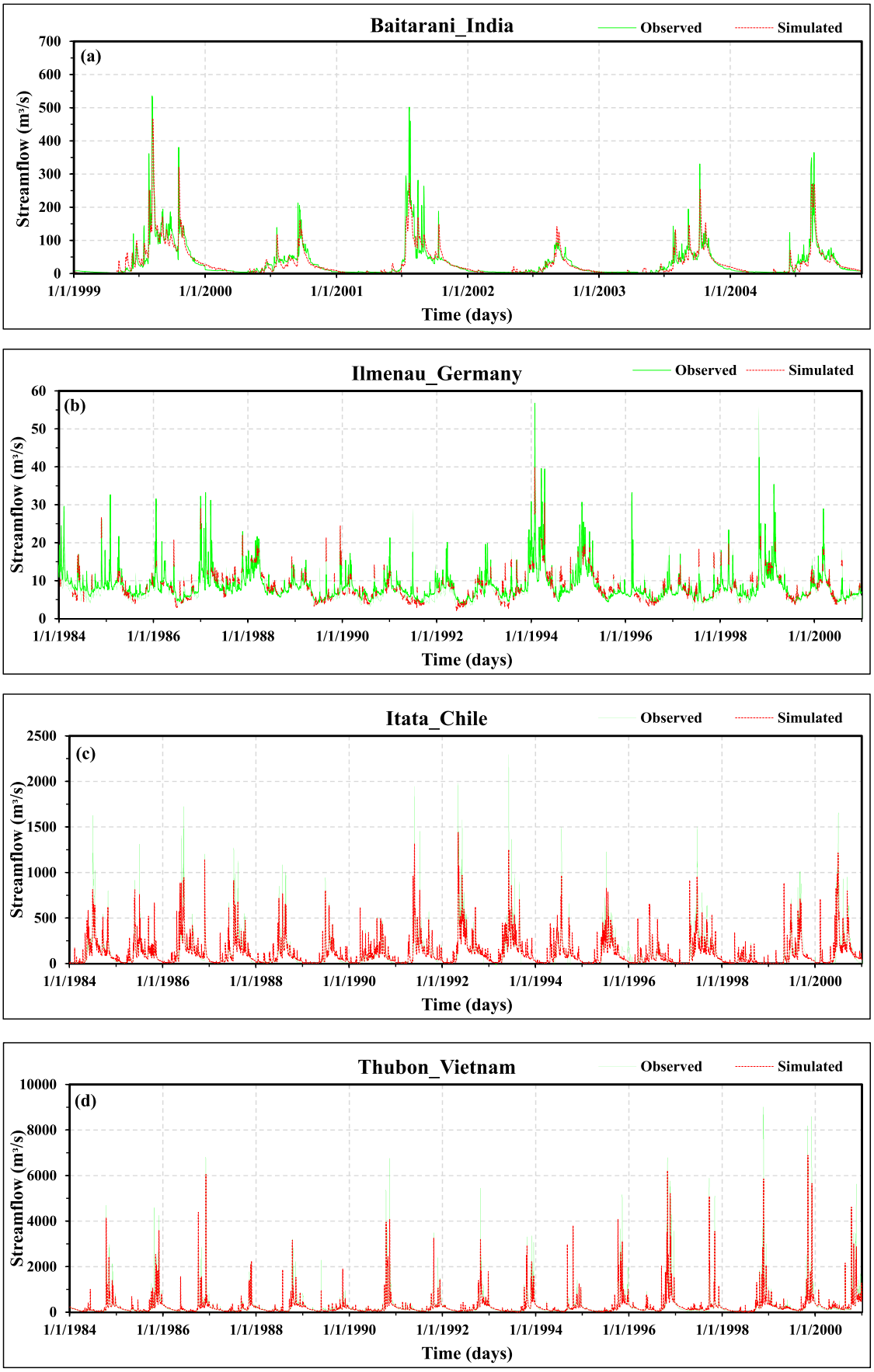

Fig. 2. (a–d). Streamflow hydrographs for the four catchments during their respective calibration periods.

Table 2
Model evaluation statistics.

Catchments		Statistical indicators			
		R^2 (Coefficient of determination)	NSE (Nash-Sutcliffe efficiency)	PBIAS (%, percent bias)	KGE (Kling-Gupta efficiency)
Baitarani	Calibration (1999–2004)	0.81	0.81	6.90	0.89
	Validation (2005–2010)	0.60	0.60	−3.23	0.76
Ilmenau	Calibration (1981–2000)	0.65	0.62	1.18	0.80
	Validation (2001−2010)	0.61	0.51	3.46	0.76
Itata	Calibration (1984–2000)	0.68	0.68	3.39	0.74
	Validation (2001–2010)	0.70	0.70	−7.02	0.80
Thubon	Calibration (1984–2000)	0.85	0.84	4.98	0.81
	Validation (2001–2010)	0.88	0.87	1.39	0.87

level. An HRU is the unique combination of soil, land use and slope within a sub-basin.

3.2. Crop model setup

SWAT uses a simplified version of the crop growth model used in EPIC (Neitsch et al., 2011). It uses the same crop growth equations for all the crops but each crop has unique values for the model parameters. In this way, the crop growth model differentiates between different crops. Plant growth is calculated by simulating leaf area development, interception of light and its conversion into biomass. Crop yield is a function of biomass above ground and harvest index on the day of harvesting. In addition, biomass on a day depends on the total intercepted solar radiation and also on leaf area index, whereas the harvest index depends on the accumulated heat units. Heat units are climate based mechanism to grow crops according to thermal input and to initiate irrigation and fertilizer application in the model. Crops grow if the accumulated temperature above a threshold value reaches to a user defined value. SWAT categorizes plants into seven different types based on the season (cold or warm), type (legumes/others), growing period (seasonal, annual or perennial) and trees (Neitsch et al., 2011).

Latest available crop statistics at district or regional level was incorporated into the models. Different crop types were randomly distributed in the agricultural areas of the respective basins using their respective percentage of the total agricultural area determined by GIS overlay analysis. However, in case of Baitarni river basin the state crop statistics were taken to distribute crops in the agricultural area. Through this, all the catchments show average crop spatial statistics according to the recent census. As fixed operations under local conditions were not available, therefore the developed models mostly depend on climate input data. The crops in all the catchments were grown using heat units. Auto-fertilization was activated, so there was no nutrient stress. Harvesting is done by using 'harvest and kill function' or by using 'harvest only' function. The 'harvest and kill' function harvests the plant biomass and kills the crop upon harvest whereas the other only harvests the crop, but allows the plant to continue growing. One crop is grown in the model in a year. However, in case of Thubon rice is grown twice a year. The possible intermediate crops are neglected because they are mostly not irrigated if grown. Forest and range land are modelled as perennial plants in the catchment.

3.3. Implementation of irrigation schemes

SWAT does not regard the method of irrigation directly. Only the losses associated with the different methods of irrigation can be given via parameters called surface runoff ratio (IRR_ASQ) and irrigation efficiency (IRR_EFF; amount of water which is completely lost from the system). Therefore, the user can assign the overall water loss from the system (e.g. leaching, evapotranspiration) by the parameter IRR_EFF, whereas IRR_ASQ is used to implement the return flow occurring from the surface runoff to the system. Values for the irrigation system efficiency for different irrigation techniques were taken from the Food and Agricultural Organization database (http://www.fao.org/docrep/t7202e/t7202e08.htm).

Nearly 85% of the irrigation demand is satisfied from surface water in the Baitarani River basin. According to FAO, only 3.2% of the agricultural area in Chile is irrigated by using groundwater (http://www.fao.org/nr/water/aquastat/irrigationmap/CHL/index.stm). In Vietnam, total

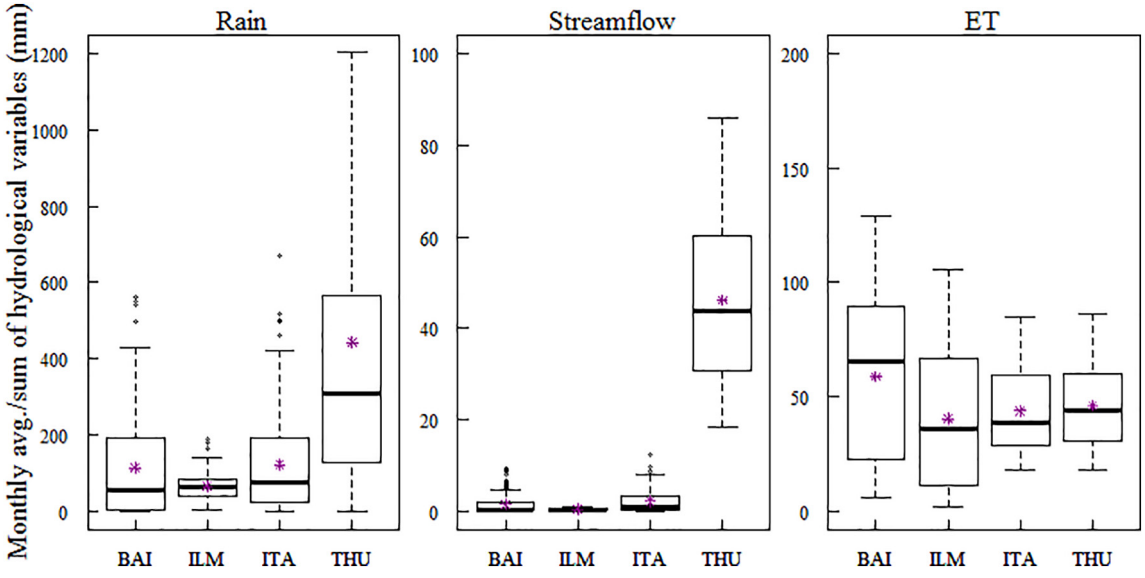

Fig. 3. Main water balance components of the different catchments. *Asterisk shows the average values. The abbreviations used are as follows-BAI: Baitarani, ILM: Ilmenau, ITA: Itata and THU: Thubon.

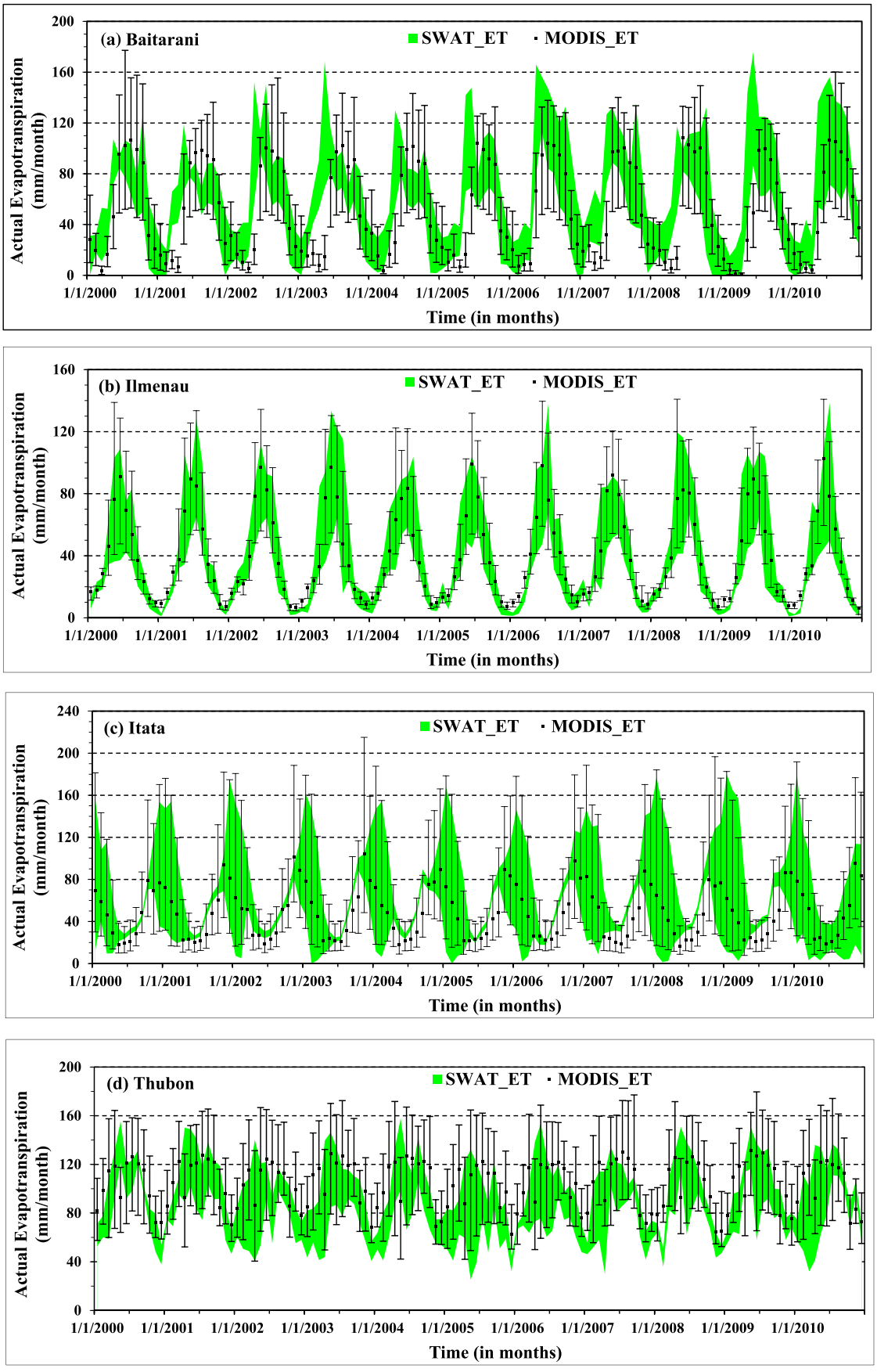

Fig. 4. (a–d). Spatio-temporal variation of actual evapotranspiration in (a) Baitarani; (b) Ilmenau; (c) Itata and (d) Thubon from 2000 to 2010 at monthly time step. *Green band shows the range of ET in the entire agricultural area of the catchment.

Table 3
Comparison of crop yield.

Catchment	Type of crop	Crop yield (dry, t/ha)	
		Simulated	Statistics
1. Baitarni	Rice	2–2.4	1.1–2.5[b]
2. Ilmenau	Potato	6.4–7.3	7.7–8.5[c]
	Sugarbeet	8.1–11.1	9.8–11.2[c]
	Winter Wheat	5.4–5.8	5.7–6.9[c]
3. Itata	Oats	4.1–4.3	2.7–5.3[a]
	Winter Wheat	2.5–6.6	2.1–6.9[a]
4. Thubon	Rice	1.6-5.4	~5[d]

[a] Average crop statistics of the whole country, Chile (FAO) 1980–2010.
[b] Technical rice report of Odisha 1980–2010 and Keonjhar 2005.
[c] Niedersächsisches Landesamt für Statistik 1990–2000.
[d] Firoz et al., 2018.

groundwater withdrawal is only 1.7%, which is mainly used for supplying municipal water to the urban areas (http://www.fao.org/nr/water/aquastat/countriesregions/VNM/). This justifies the use of surface water for irrigation in Baitarani, Itata and Thubon catchments. For Ilmenau River basin, only groundwater was used as the source of irrigation water.

3.4. Irrigation scheduling

Irrigation operations can be initiated in SWAT either by the predefined schedules or automatically based on climate and plant growth using heat units. Automatic irrigation can be triggered by defining plant water stress or soil water deficit threshold in the model (AUTO_WSTR: water stress threshold). If irrigation is triggered by plant water stress, then the water stress threshold is a fraction of potential plant growth. Plant water stress is simulated in SWAT by a comparison of actual and potential plant transpiration:

$$wstr = 1 - \frac{E_{t,act}}{E_t} = 1 - \frac{w_{actualup}}{E_t} \quad (1)$$

where, *wstr* is the water stress, E_t is the maximum plant transpiration, $E_{t,act}$ is the actual amount of transpiration and $w_{actualup}$ is the total plant water uptake.

The irrigation source has to be defined on a sub-basin level like reach, reservoir, shallow and deep aquifer, etc. Automatic irrigation adds water until the field capacity of the soil profile (root zone) is reached and the excess water returns to the source.

When water stress is based on the soil water deficit, the water stress threshold is the soil water deficit below field capacity (mm H_2O). Whenever the water content of the soil profile falls below FC (field capacity) – AUTO_WSTR [the acceptable amount of water depletion (mm H_2O) in the total soil column], the model will automatically apply water to the HRU. If enough water is available from the irrigation source, the model will add water to the soil until it is at FC (Neitsch et al., 2011). Considering the vertical and horizontal heterogeneity of FC, the individual soil water depletion (AUTO_WSTR) values for different soil and crop types have to be quantified. In all the calibrated SWAT models, automatic irrigation was scheduled by using plant water stress.

All the developed models were calibrated using streamflow observed at the catchment's outlet. For the Ilmenau and Itata catchments, streamflow data from intermediate stream gauging stations were used to improve the calibration. All of the developed models were iteratively calibrated by using manual as well as automatic techniques along with local expert knowledge about the four catchments. Nash Sutcliffe efficiency (NSE > 0.5) and percentage bias (PBIAS <10%) were used as objective functions to calibrate the developed models.

In addition, the SWAT simulated ET was compared with ET extracted from MODIS for all the four catchments on monthly basis and for all agricultural HRUs during 2000–2010. In order to compare the overall spatial and temporal variation in SWAT simulated ET with MODIS, ET bands were created from the minimum, maximum and average values of ET for a particular month from the agricultural HRUs.

3.5. Irrigation scheduling scenarios

For the scenario simulations, two different irrigation scenarios (optimal and deficit irrigation) were used for scheduling irrigation for both plant water stress and soil water deficit with different thresholds. For

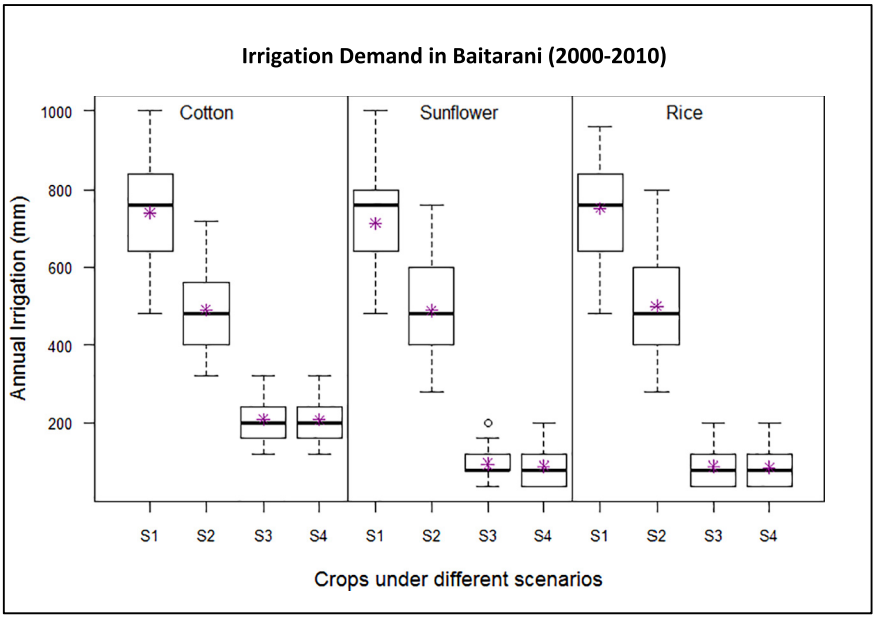

Fig. 5. Spatio-temporal variation of simulated annual Irrigation in Baitarani under different irrigation scenarios from 2000 to 2010. *(asterisk) shows the mean annual irrigation demand during 2000–2010.

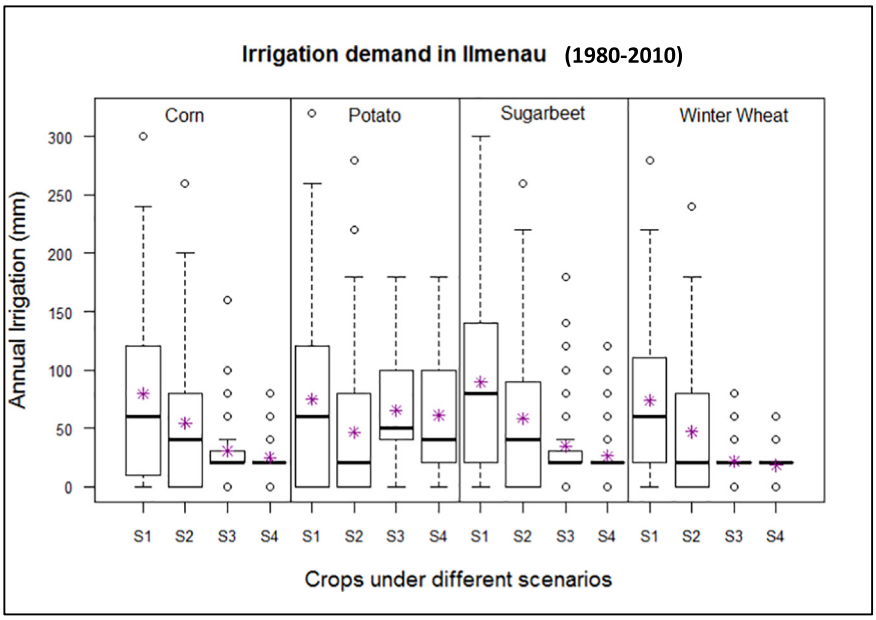

Fig. 6. Spatio-temporal variation of simulated annual Irrigation in Ilmenau under different irrigation scenarios from 1980 to 2010. *(asterisk) shows the mean annual irrigation demand during 1980–2010.

soil water deficit scheduling, the optimal scenario irrigates when moisture content in the soil falls below FC – 0.5∗FC in mm (scenario 1-S1) and the deficit scenario irrigates when soil moisture falls below FC – 0.65∗FC in mm (scenario 2-S2). For the plant water stress scenarios, threshold values of 0.9 (scenario 3-S3) and 0.8 (scenario 4-S4) were chosen for scheduling irrigation in all the catchments.

3.6. Application of climate reanalysis data in simulating streamflow and irrigation

Climate reanalysis simulations aim at providing climate data for unobserved or insufficiently monitored regions of the world. However, these data can be biased against climate observations (Hwang et al., 2014). Therefore, after comparing the reanalysis datasets (NCEP and ERA) with observed values used in this study, daily precipitation, temperature (minimum and maximum) and solar radiation were bias corrected by using quantile mapping (Piani et al., 2010a; Piani et al., 2010b; Thrasher et al., 2012). The bias correction is performed to reduce the effect of local over or underestimation of climate variables by the global models (Varis et al., 2004; Christensen et al., 2008; Teutschbein and Seibert, 2010). Quantile mapping was conducted using the R statistical tool package 'qmap'. This program first estimates the empirical cumulative distribution function of the observed and reanalysis data for 10 quantiles and derives a transformation function for each quantile. Later

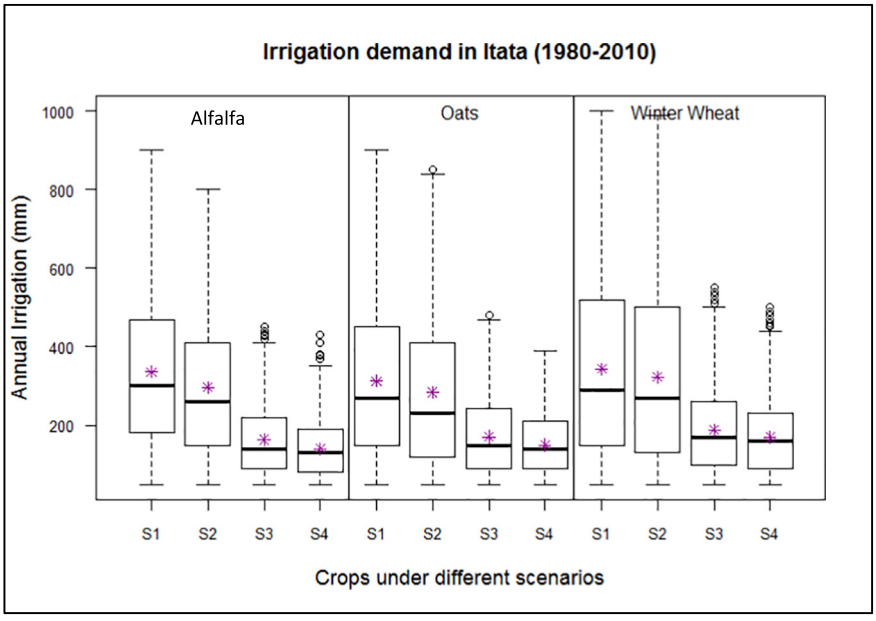

Fig. 7. Spatio-temporal variation of simulated annual Irrigation in Itata under different irrigation scenarios from 1980 to 2010. *(asterisk) shows the mean annual irrigation demand during 1980–2010.

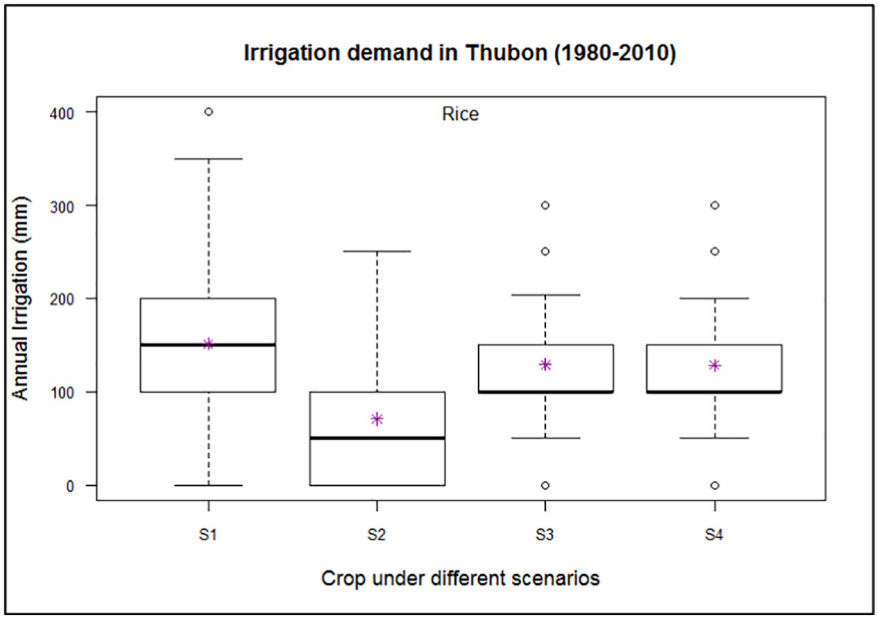

Fig. 8. Spatio-temporal variation of simulated Irrigation in Thubon under different irrigation scenarios from 1980 to 2010 at yearly time step. *(asterisk) shows the mean annual irrigation demand during 1980–2010.

on, the quantiles of the original reanalysis dataset are transformed into the quantiles of the bias corrected dataset. For the values that are outside of the fitted distribution function, their transformation is estimated by using spline interpolation (ftp://ftp.gr.vim.org/mirrors/CRAN/web/packages/qmap/qmap.pdf). For this study, month specific bias correction for daily weather variables was selected due to the significant difference in the seasonal rainfall patterns. The observed data were replaced with the reanalysis dataset in the developed models to evaluate their performance, assuming that the model calibration with observed data is valid i.e., representing the hydrological system response to climatic forces. The accuracy of simulations with bias corrected and uncorrected reanalysis climate data was tested against simulations with observed climate data for the four catchments.

4. Results and discussion

4.1. Calibration and validation of SWAT

All the selected catchments were calibrated using the daily streamflow at their respective outlets. The streamflow hydrographs of the selected catchments are shown in Fig. 2(a–d) for the respective calibration periods. It can be seen that the calibrated models replicate the range of values of streamflow hydrographs during the calibration period in all the catchments with different performance. Overall, it can be assessed from the hydrographs that SWAT consistently underestimates the peak flows as compared to the low flows and recession limbs, which are well replicated. This can also be seen from the flow duration curves, which are shown in Section 4.5. The daily hydrograph simulated by SWAT can underestimate the peak if the travel time is less than one day as this is a limitation of the Muskingum's routing equation used in the model (Kim and Lee, 2010). Furthermore, the available weather stations might not be enough to represent the overall spatial variability of local events in the catchments. The Kling-Gupta Efficiency (KGE, Gupta et al., 2009) varies from 0.74 to 0.89 and the percentage bias (PBIAS) from −7.02 to 6.9% (Table 2), which indicates a good to very good model performance according to Moriasi et al. (2007). In addition to it, Table 2 also shows the performance of SWAT models for other criteria of fit as well as the performance of the model during validation period. It shows a comparable level of performance as shown in calibration period except in case of Baitarani river basin. This is due to the poor rainfall data during the validation period (2007).

Fig. 3 shows the boxplots for monthly rainfall (mm), average monthly simulated streamflow (mm) and areal average actual evapotranspiration (mm) in the four studied catchments. It can be inferred from the figure that even though the overall variability in rain, ET and streamflow is huge, the average values of precipitation and stream flow are relatively close for Baitarni, Ilmenau and Itata, whereas the tropical catchment of Thubon shows a different characteristic. A direct relation can be seen between rainfall and streamflow in all the catchments. A nonlinear relation between rainfall and streamflow is seen in the tropical mountainous catchment of Thubon. The overall water yield is really high in this catchment as compared to the others. Monthly streamflow also shows clear difference between a wet tropical catchment (Thubon) and a subtropical catchment (Baitarni), even the low flows in the Thubon catchment are more than the high flows in the Baitarani catchment. The overall behavior of monthly average ET can provide information about the climate of a respective catchment. It can be seen from the ET boxplots that overall spreads of the Baitarni and Ilmenau catchments are more than that of the Itata and Thubon catchments. The wide spread of ET in the Baitarani catchment support its subtropical climatic characteristic with defined winter, summer and monsoon season and in case of the Ilmenau catchment, it shows its distinct summer and winter season. In addition, the ET boxplots show an increasing gradient towards the equator from Ilmenau to Thubon with a bigger step in Baitarani catchment. However, the overall spread and monthly average ET for Thubon is expected to be higher but SWAT has been reported to underestimate ET of tropical evergreen forests systematically (Plesca et al., 2012; Alemayehu et al., 2017).

4.2. Evaluation of simulated evapotranspiration and yield for agricultural land use

The spatio-temporal comparison of monthly ET from MODIS and SWAT was performed for the four catchments during 2000 to 2010. The overall spread from MODIS data was plotted with the simulated ET band from SWAT. It can be seen from Fig. 4(a–d) that even though the overall spread of monthly ET from MODIS and SWAT is not exactly matching, the overall dynamics is similar in both datasets for all the four catchments. In addition to it, the mean ET from MODIS mostly

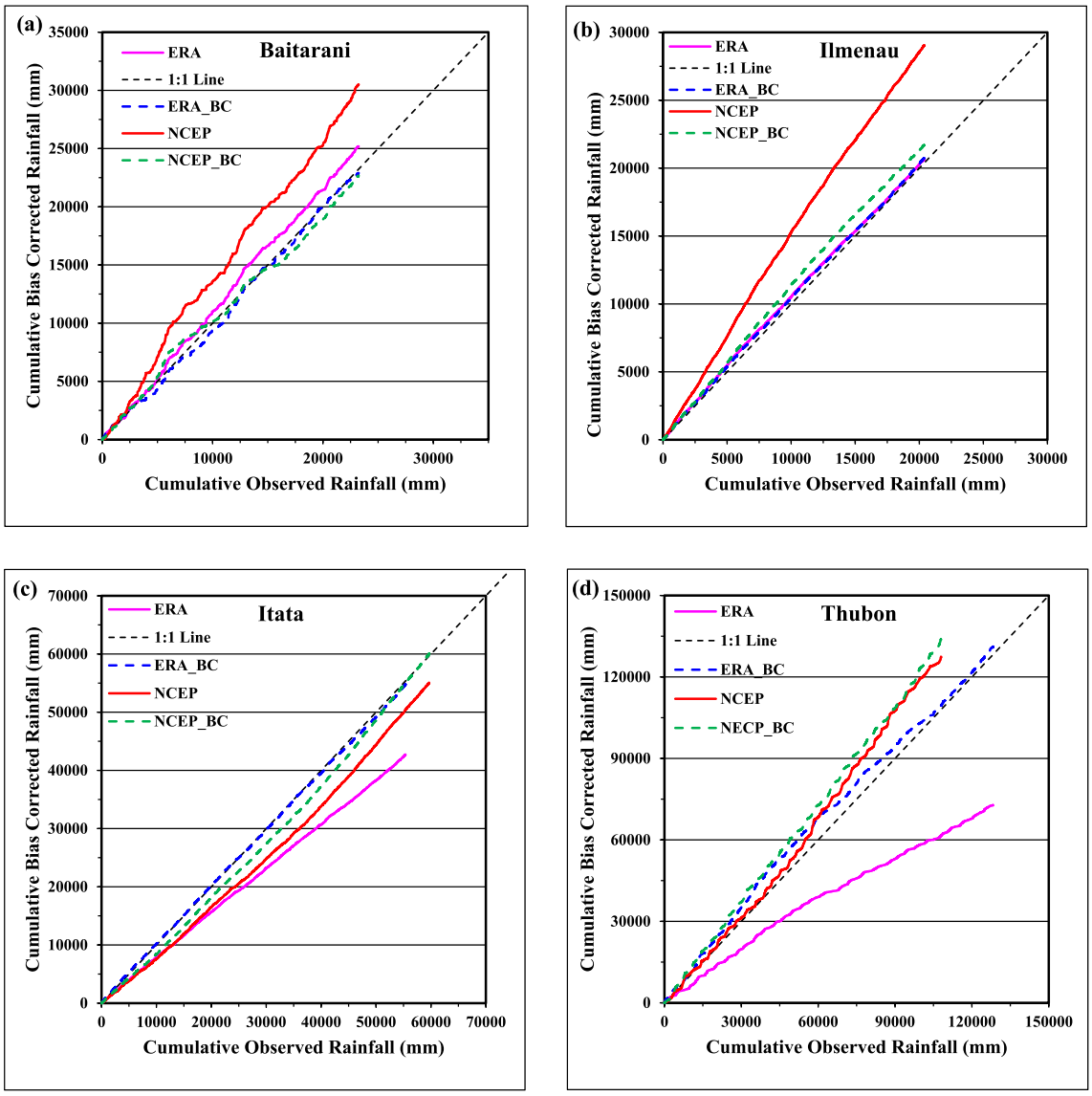

Fig. 9. Double mass curve of long term rainfall data for (a) Baitarani, (b) Ilmenau, (c) Itata, (d) Thubon.

falls inside the simulated ET band from SWAT. However, SWAT simulates higher ET as compared to MODIS by 3 to 20% in the Baitarani, Ilmenau and Itata catchments, whereas lower ET in case of Thubon (~25%). It can be seen that during the growing period, the spread is wide in both cases and narrows down during non-growing periods. Statistical results showed that the percentage deviation in mean monthly ET estimated for SWAT and MODIS has different behavior for different catchments. This might be due to the difference in topography and climatic conditions of the respective catchments. It can be seen from Fig. 4(a) that for the Ilmenau catchment, the overall spread of the estimated and simulated ET matched well as compared to the other catchments. This can be attributed to the good water balance simulated by SWAT in this basin because it was calibrated by using three more intermediate stations apart from the outlet. The data quality and quantity play a crucial role in this context.

Table 4
Statistical evaluation of daily reanalysis rainfall.

Sl. no.	Catchment	Statistical indicators (1980–2010)	NCEP	NCEP_BC	ERA	ERA_BC
1.	[a]Baitarani	PBIAS (%)	−27.28	5.66	−9.44	−1.85
		MAE (daily, mm)	5.23	4.86	4.70	5.0
2.	Ilmenau	PBIAS (%)	−42.44	−6.43	−1.32	−1.8
		MAE (daily, mm)	2.25	1.97	1.40	1.47
3.	Itata	PBIAS (%)	7.74	−0.67	28.39	8.19
		MAE (daily, mm)	5.32	5.45	7.71	4.19
4.	Thubon	PBIAS (%)	15.21	−5.27	43.32	−1.69
		MAE (daily, mm)	11.99	12.02	10.67	11.43

[a] Analysis for Baitarani river basin has been carried out from 1998 to 2010.

Fig. 4(b) shows that the ET estimated from MODIS data for the Baitarani river basin during March–May is lower than the simulated ET from SWAT. It is also apparent that the period of plant growth and the receipt of rainfall for this catchment is in the same period. Therefore, with the available justification and local knowledge about the area, it can be concluded that MODIS is underestimating ET for this catchment.

It can be seen from Fig. 4 (c) that the overall variation in ET simulated by SWAT and MODIS is high in the Itata catchment during April–October. This is explained by the inclusion of agro-forest under agricultural land. This is confirmed by evaluating the Google earth imagery with the agricultural area of the Itata catchment. In addition to this, during this period Chile experiences winter and growing crops are not generally favored in this tenure.

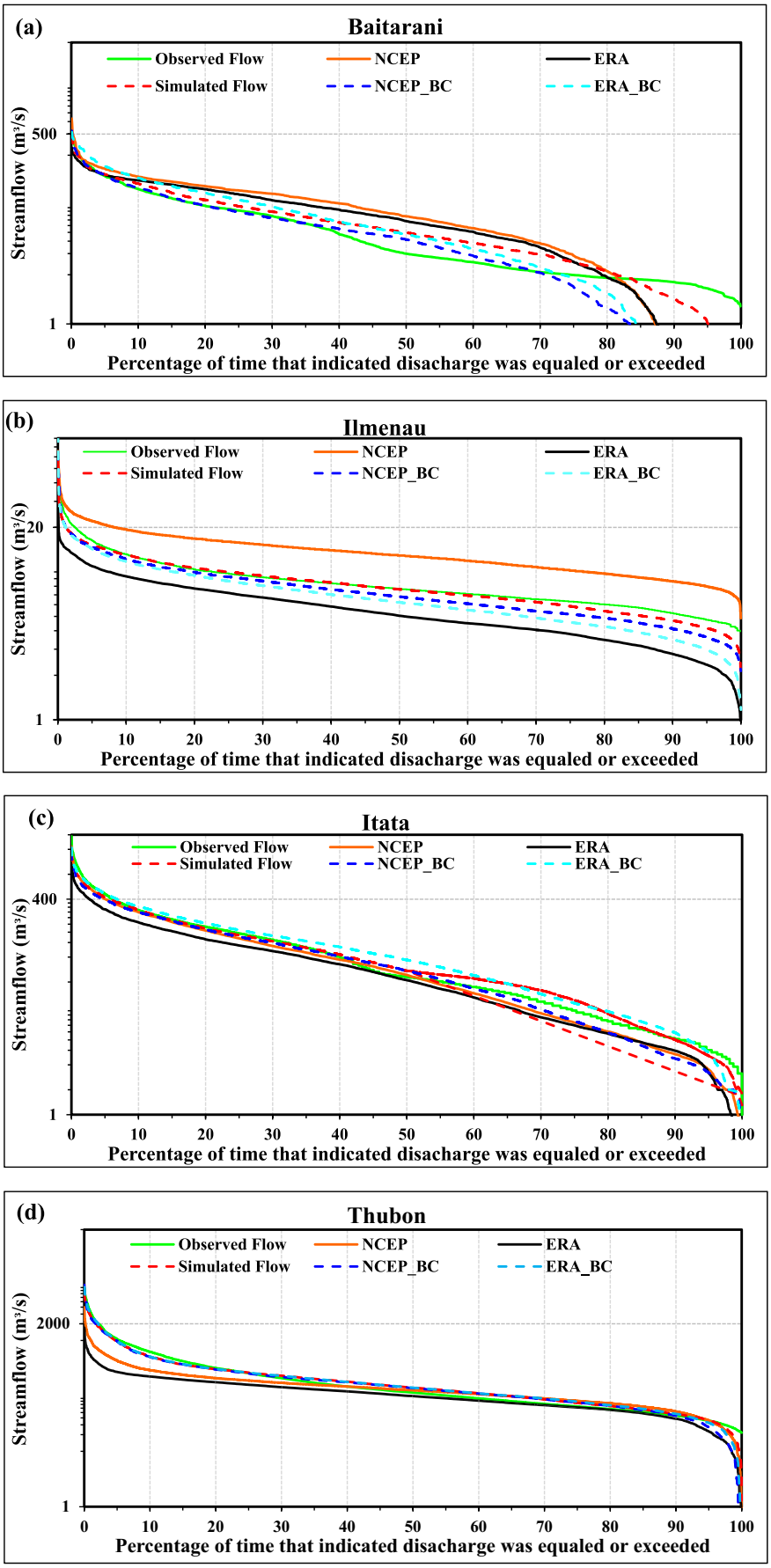

Fig. 10. Flow duration curves for the calibration period in (a) Baitarani, (b) Ilmenau, (c) Itata, (d) Thubon catchments.

Table 5
Statistical evaluation for checking the application of reanalysis datasets for simulating streamflow.

Sl. no.	Catchment	Statistical indicators (1984–2000)	NCEP	NCEP_BC	ERA	ERA_BC
1.	Baitarani[a]	PBIAS (%)	−30.28	24.88	−31.89	−8.61
		KGE	0.37	0.30	0.53	0.46
		R^2	0.22	0.13	0.44	0.27
2.	Ilmenau	PBIAS (%)	−52.99	11.83	40.38	18.65
		KGE	0.36	0.63	0.42	0.622
		R^2	0.47	0.42	0.56	0.45
3.	Itata	PBIAS (%)	16.35	12.36	31.68	−6.88
		KGE	0.75	0.72	0.49	0.82
		R^2	0.70	0.72	0.76	0.77
4.	Thubon	PBIAS (%)	39.4	6.54	54.04	2.25
		KGE	0.14	0.71	−0.05	0.67
		R^2	0.44	0.57	0.41	0.45

[a] (Asterisk) streamflow simulation during 1999–2005.

In Thubon catchment (Fig. 4(d)), the overall spread and mean values of estimated ET from MODIS are larger than that of the simulated ET in SWAT. Two plausible reasons for this result are: a) SWAT underestimates actual ET from the highly saturated agricultural surface by limiting ET to potential ET (Neitsch et al., 2011), whereas in the case of rice production actual ET can be more than potential ET as described for ponds by Xie and Cui (2011), and b) the parameters for the crop varieties could not be calibrated for the local conditions. Hai (2003) confirmed that Vietnam uses hybrid rice varieties (high yielding varieties), which consume more water and in turn might have more ET than the standard varieties as included in the SWAT database.

The ET estimated by MODIS also has some uncertainty as the meteorological data used in the estimation of MODIS ET is non-linearly interpolated as it was too coarse for one MODIS pixel (Mu et al., 2013). The aforementioned interpolation is assumed to improve the ET calculations, however, there is also some uncertainty at local scale.

The crop yield was not used to calibrate the models in this study, because local data were not available. For evaluating the plausibility of the obtained yield, Table 3 show the overall range of the annual yield as simulated by SWAT for main crops compared to publicly accessible crop statistics from census data. It can be seen from this table that even though the range is matching for most of the catchments, still there is huge uncertainty in simulated yield as well as the statistics used for comparison. In general, it is a difficult task to calibrate yield due to input data limitations in terms of planting and harvesting dates, fertilizer and water inputs (quantity and frequency of application), losses due to pests, floods and droughts etc. The reported model uncertainty can be due to input data, model parameters as well as the climatic variation during the simulation period. Authors accept this uncertainty as they are in similar ranges as other studies have shown, e.g. Abbaspour et al. (2015).

4.3. Comparison of different irrigation control scenarios

This section explains the results corresponding to different irrigation control scenarios used in the current study for simulating annual irrigation water requirement for major crops growing in the different catchments. Fig. 5 shows the average annual irrigation demand of cotton, sunflower and rice in the Baitarani River basin for the 2000–2010 period. It can be seen that the average annual irrigation water provided by the model is approximately two times more in the case of soil-water deficit scenarios (S1 and S2) compared to the plant-water stress scenarios (S3 and S4). The annual average water requirements under soil-water deficit scenarios are in accordance with the annual irrigation water applied in the field during conventional planting of rice (Nayak, 2006). Due to the scarcity of literature in this catchment for the actual amount of water applied to cotton and sunflower production, the simulated results cannot be validated against observed data or previous modelling studies. Sunflower is grown in Kharif season (during July–December) as well as in Rabi season (summer). It requires no irrigation during winter season. However, if it is grown in non-rainy seasons then around 500–1000 mm irrigation water is required depending on the soil type. The crop (sunflower) is growing in summer season in the developed model. Therefore, the irrigation water simulated by SWAT is justified (100–700 mm). The change in overall yield has also been analyzed under the four irrigation scenarios, which was found to be <10% in plant-water stress irrigation control scenarios as compared to the soil-water deficit scenarios. However, water saving is nearly equal to 50% if the soil water deficit scenario (S2) is used with minimal change in the annual average yield.

The irrigation water depth for the Ilmenau region is limited to 70 mm per summer over a seven-year average, i.e., higher abstractions in dry years can be compensated by lower ones in wet summers (Wittenberg, 2015). It can be assessed from Fig. 6 that the annual average irrigation water requirement simulated by the model under considered management scenarios is <100 mm. In addition to it, under different water application scenarios the amount of irrigation simulated by the model under optimal scenario is 2 to 1.5 times more than the deficit scenario in case of Corn, Sugar beet and Winter wheat. Under S3 and S4 scenarios, the net reduction in the crop yield (Corn, Potato, Sugar beet and Winter wheat) varies from 0.23% (Sugar beet) to 10% (Potato). It can be seen that the water demanding crops have more variation in their yield than the low water demanding crops under different water scheduling scenarios.

Fig. 7 shows the annual average irrigation applied in the Itata catchment for Alfalfa, Oats and Winter wheat during 1980 to 2010. There is very few literature available to validate the amount of irrigation simulated by the model. In addition to this, there are several HRUs in which the crop yield is relatively low or zero as compared to the mean yield (4.5 t/ha). It might be due to the very small HRU size and due to the small depth of soil profile in some soils. The amount of irrigation water applied by the model in case of winter wheat is in accordance with the experiment conducted by Vidal et al. (1999), in which they applied 225–880 mm of irrigation in four steps. Due to the scarcity of literature for the actual amount of water applied in Oats and Alfalfa crops, we cannot exactly validate the results against observed data or previous modelling studies.

The average annual irrigation in Vietnam is around 400 mm but supplemental irrigation can vary from 80 to 400 mm (Shrestha et al., 2016), which is within the annual irrigation range simulated by SWAT during 1981–2010 (Fig. 8). The difference in the annual average crop yield is <5% under soil water deficit and plant water scenarios. The average simulated irrigation water demand is lower than the country's average water demand. This might be due the reason that the rice yield (Avg. yield = 4.0 t/ha, range: 1.6–5.4 t/ha) simulated by the SWAT model is relatively low in some HRU's as compared to the country's average rice yield (~5 t/ha, Firoz et al., 2018). This low rice yield could be attributed to some really small HRU's which are not well simulated by the model or different high yielding rice varieties currently used in the country whose plant parameters are entirely different from the one (generic rice) used in SWAT (Hai, 2003; Ut and Kajisa, 2006).

4.4. Correction of reanalysis data

The climate reanalysis data (rainfall, maximum, minimum temperature and solar radiation) has been corrected using quantile mapping as mentioned in Section 3.6. The results corresponding to bias corrected rainfall are shown in this section. The double mass curve technique is used to check the consistency of long-term precipitation data for one selected station in all the four catchments (Searcy and Hardison, 1960). Fig. 9 shows double mass curves of the uncorrected and bias corrected re-analysis data against the observed rainfall for the Baitarani, Ilmenau, Itata and Thubon, catchments, respectively. The aforementioned curves

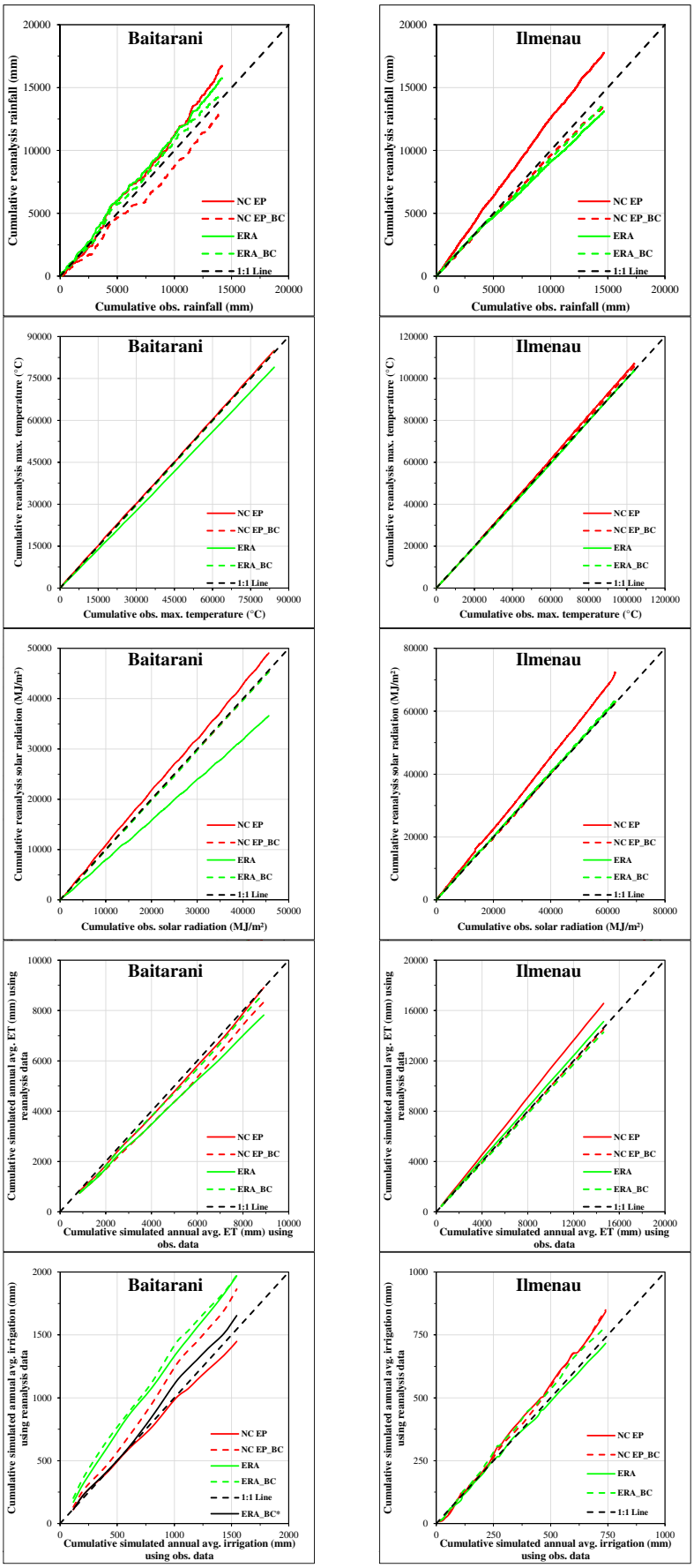

Fig. 11. Double mass curves for different climate variables, simulated annual average ET and irrigation for observed and reanalysis datasets for (a) Baitarani, (b) Ilmenau, (c) Itata, (d) Thubon catchments, respectively. *ERA_BC* is the annual average irrigation simulated by using bias corrected rainfall, solar radiation and uncorrected temperature data.

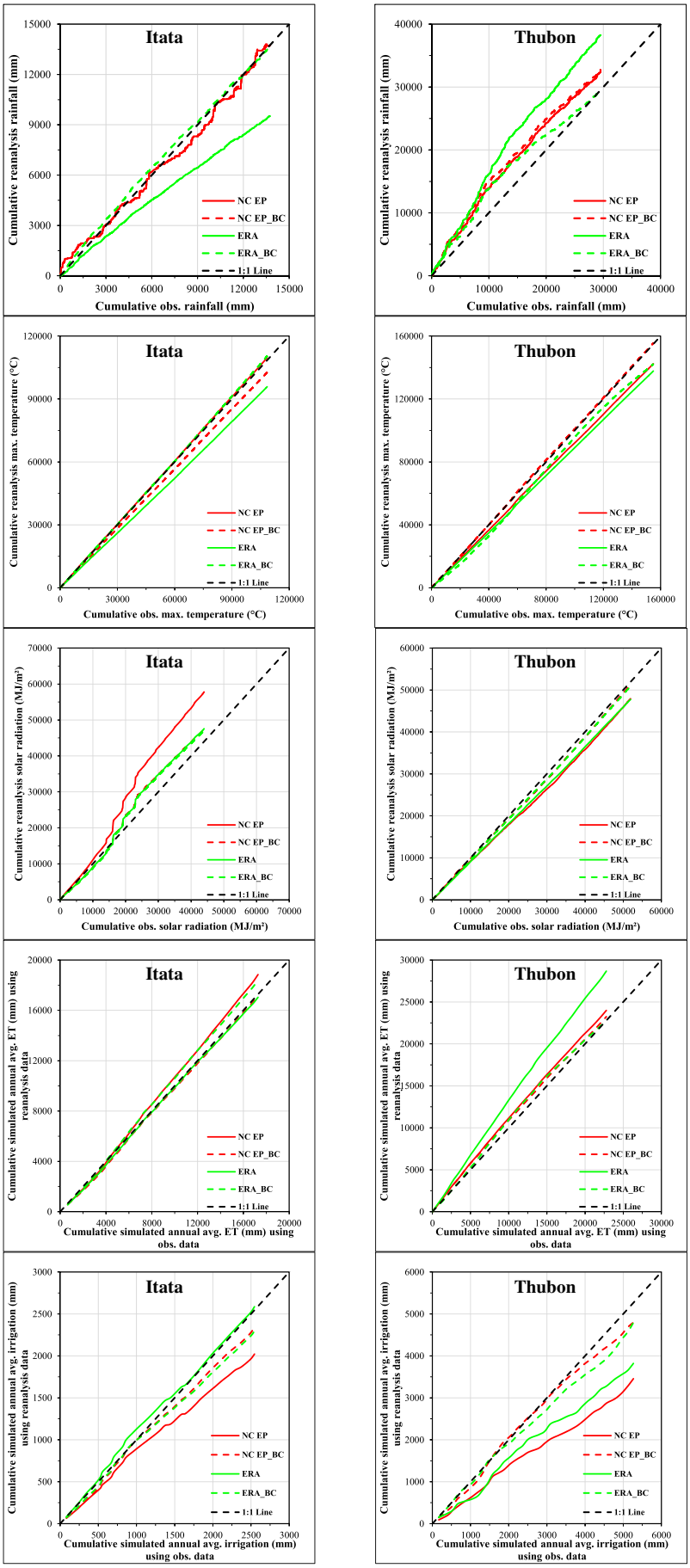

Fig. 11 (*continued.*)

are drawn for 1980 to 2010 for all the catchments except Baitarani (1998–2010) due to observed data constraints. It can be seen from Fig. 9 that uncorrected rainfall show different response from NCEP and ERA compared to the observed in a catchment. This is due to the different spatial resolution as well as the different atmospheric, ocean and land surface models used to estimate the climate variables of the two reanalysis datasets. In addition to this, it is very interesting to see that e.g., ERA has overestimated the rainfall in the Baitarani and Ilmenau catchments, whereas it was underestimated in the other two catchments. The overall behavior of observed rainfall after the bias correction is reproduced well (Fig. 9). As the correction is done for all the months separately, the program tries to match the overall behavior as well as the amount of bias corrected rainfall with the observed rainfall. In addition to it, the correction gave a relatively good result describing the seasonal or monthly patterns of the rainfall dataset. This can be seen in almost all the cases depicted in Fig. 9. All the bias corrected datasets are close to the 1:1 line as compared to their respective uncorrected datasets. Apart from the qualitative assessment, quantitative assessment of the bias corrected ERA and NCEP datasets is also performed (Table 4). It can be seen from the statistics that the PBIAS and mean absolute error (MAE) has improved in case of bias corrected data. In addition to this, it is clear from the analysis that the bias corrected ERA interim datasets are more close to observed rainfall than NCEP. It must be mentioned that the bias correction has not worked well for some daily rainfall values, which might influence the final result of the developed SWAT models. Thus, more investigation should be taken into account while analyzing the final model simulation using the reanalysis datasets. In addition to this, it can be seen from Table 4 that quantile mapping is unable to reduce the bias to zero. Although the overall bias is always less than ±15% in bias corrected rainfall datasets.

4.5. Forcing streamflow and irrigation simulations with climate reanalysis data

The application of uncorrected and bias corrected reanalysis data for simulating streamflow is evaluated by using the flow duration curves (Fig. 10(a–d)) as well as model evaluation statistics (Table 5). In this research, more interest was given to evaluate the low and mean flows as this plays a major role in the irrigation season. It can be seen from the flow duration curves drawn from the four catchments under bias corrected and uncorrected cases (NCEP and ERA) that the simulated streamflows under bias corrected climate data are close to the observed streamflows. In addition to this, it is clear from the quantitative assessment conducted on daily time step that the streamflow simulated by using bias corrected data are usually better when compared to the observed streamflow than the streamflow simulated using uncorrected data (Table 5). It can be seen from Table 5 that the streamflow simulated by using bias corrected ERA data (ERA_BC) with PBIAS: −8.61–18.65% and KGE: 0.46–0.67 is better than the streamflow simulated by using bias corrected NCEP data (ERA_BC), which has PBIAS: 6.54–24.88% and KGE: 0.30–0.72. In addition to this, it can be assessed from the aforementioned table that streamflow simulated by using uncorrected NCEP data does not yield satisfactory results for all the four catchments, whereas the streamflow simulated using uncorrected ERA has acceptable to satisfactory values in Baitarani, Ilmenau and Itata catchments. Therefore, it can be inferred from the results that the uncorrected reanalysis data is highly uncertain to streamflow simulation in all the catchments of this study. However, it can be concluded that bias correction allows good performance of the hydrological model driven by reanalysis datasets. In addition to this, ERA uncorrected data can also be useful in filling the data gaps of the data scarce catchments or can be used as a proxy for the catchments where input data is not at all available.

Apart from evaluating the performance of reanalysis datasets in simulating streamflow in the four catchments, the annual average evapotranspiration and irrigation are also evaluated. As observed irrigation values were not available for all the catchments, the simulated irrigation using observed climate data is compared with the corresponding simulated irrigation using uncorrected and bias corrected climate reanalysis datasets for the catchments. Double mass curves are drawn for average annual simulated irrigation under observed and reanalysis datasets. In general, it can be seen from Fig. 11(a–d) that irrigation simulated by using the bias corrected data is closer to the 1:1 line as compared to using the uncorrected reanalysis (NCEP and ERA) data in most cases. The percentage deviation in the irrigation simulated using reanalysis data from the simulated irrigation under observed data is shown in Table 6. It can be seen that the long-term average simulated irrigation percent deviation under different cases varies from −27.51 to 75.66%. The aforementioned results are backed by a study performed by Wisser et al. (2008), which states that the error in simulating the irrigation water demand can be as high as ±70% at national scale. In addition to this, it can be seen from the results that the simulated irrigation is sensitive to different weather variables or combination of weather variables in different catchments. As shown in Fig. 11, the rainfall in case of the Thubon model (sensitive to rainfall) is overestimated compared to the observed rainfall and this leads to the underestimation of simulated irrigation water demand in NCEP and ERA. However, this is not valid in case of the Baitarani catchment. Furthermore, the annual average simulated irrigation in case of bias corrected ERA (ERA_BC) is closer to the simulated irrigation under observed data (percent deviation: −7.03–8.89%) in almost all the cases except Baitarani (percent deviation: −20.63%). This deviation in simulated irrigation using bias corrected weather dataset can be due to the reason that the bias corrected minimum temperature is not meeting the temporal variability because there is only one temperature gauging station. However, the deviation was acceptable when the model was rerun by only using bias corrected rainfall and solar radiation. In this case the model gave acceptable results as shown in Fig. 11 indicated by ERA_BC* (percent deviation = −7.02%). Additionally, the double mass curves of areal average rainfall, average maximum temperature and solar radiation are also evaluated during the cropping season against the model simulated annual average evapotranspiration and irrigation for reanalysis datasets. The aforementioned figures confirm the importance of investigating and correcting the bias in temperature and solar radiation as they also play a role in simulation of irrigation water requirement as much as rainfall variability. It can be seen from Fig. 11 that the simulated ET is directly related to the overestimation and underestimation of rainfall by reanalysis data compared to the observed rainfall.

Table 7 summarizes the findings from the double mass curves of observed areal average rainfall, maximum temperature, and solar radiation during the plant growth period (Fig. 10) in order to check the plausibility of the simulated irrigation. The qualitative behavior of the aforementioned climate variables was compared in response to the simulated actual evapotranspiration and irrigation. For rainfall, maximum temperature and solar radiation table shows if the variable from reanalysis is higher (↑), lower (↓) or similar (≅) to the respective observed values in long-term average. For simulated evapotranspiration (ET) and simulated irrigation, the arrows show the results as simulated by SWAT driven with the reanalysis data. The last column of the table indicates the agreement of the simulated irrigation with the expected response. The expectation is based on the climatic feedback mechanisms with the three other variables: overestimation of rainfall can lead to

Table 6
Percentage deviation in simulated irrigation under reanalysis weather and observed weather.

Sl. no.	Catchment	Statistical indicator	NCEP	NCEP_BC	ERA	ERA_BC
1.	Baitarani	Percent deviation (%)	−27.51	−27.8	6.26	−20.63
2.	Ilmenau		−13.8	−14.6	3.24	−5.9
3.	Itata		−1.62	9.78	20.57	7.86
4.	Thubon		75.66	8.97	61.48	8.89

Table 7
Plausibility check of simulated irrigation under reanalysis climate compared to the simulated irrigation using observed data.

Catchment	Data	Rainfall	Max. temperature	Solar radiation	ET	Sim. irrigation	Agreement
Baitarani	NCEP	↑	≅	↑	≅	≅	As expected
	NCEP_BC	↓	≅	≅	≅	↑	As expected
	ERA	↑	↓	↑	↓	↑	Not expected
	ERA_BC	≅	≅	≅	≅	↑	Not expected
Ilmenau	NCEP	↑	≅	↑	↑	≅	As expected
	NCEP_BC	↓	≅	≅	≅	≅	As expected
	ERA	↓	≅	≅	↑	≅	As expected
	ERA_BC	↓	≅	≅	≅	≅	As expected
Itata	NCEP	≅	≅	↑	↑	↑	Not expected
	NCEP_BC	≅	↓	↑	↓	↓	As expected
	ERA	↓	↓	↑	↓	≅	As expected
	ERA_BC	≅	≅	↑	↑	↓	Not expected
Thubon	NCEP	↑	↓	↓	↑	↓	As expected
	NCEP_BC	↑	≅	≅	↑	↓	As expected
	ERA	↑	↓	↓	↑	↓	As expected
	ERA_BC	↑	↓	≅	↑	↓	As expected

higher ET, because more water is available for actual evapotranspiration, and lower irrigation requirement, as there is more soil water available. Higher temperature and higher solar radiation are expected to have a positive impact on evapotranspiration, which in that case will cause a higher irrigation requirement.

It is worth to mention that a clear dependency of a single weather variable to simulated irrigation is difficult to find in all the catchments as the climate variables are interdependent. In addition to this, rainfall is not always the most sensitive climate variable but it always has impact on ET.

The overall response of the simulated irrigation under different cases is also analyzed using plant and soil water stress. The areal average plant water stress for irrigated crops grown in the respective catchment area is shown in Table 8. The overall water stress in different SWAT models forced with reanalysis datasets is more than the water stress during the model developed by using the observed data except in Itata and Thubon catchments. Therefore, the model will apply more water to the crops as it can be seen in case of the Baitarani river basin for all the four cases. The aforementioned statement is also supported by the water stress days in case of the Ilmenau catchment. Considering the bias corrected data to be more close to the observed datasets, the water stress days in models forced with bias corrected weather input are closer to the ones forced with observed weather input data. In addition to this, the behavior of simulated irrigation using corrected and uncorrected reanalysis in case of Thubon can be easily justified by the water stress days in addition to the rainfall, temperature and solar radiation. As the water stress days in case of bias corrected reanalysis data is more, therefore the model applies more water, which brings the simulated values closer to the simulated irrigation under observed weather data. In addition to this, the number of water stress days when irrigation is scheduled by the soil water deficit is shown in Table 9. It can be assessed from the table that the number of stress days are higher in this case as compared to the plant water stress technique. This justifies more irrigation applied in the second case.

Table 8
Annual average water stress days for irrigated crops under plant water stress.

Sl. no.	Catchment	Observed climate	NCEP	NCEP_BC	ERA	ERA_BC
1.	Baitarani	3.8	6.2	6.1	4.7	5.6
2.	Ilmenau	0.9	1.3	1.3	1.2	1.2
3.	Itata	37.3	28.7	31.4	31	33
4.	Thubon	6.42	5.61	6.36	5.71	5.98

Table 9
Annual average water stress days for irrigated crops under soil water deficit.

Sl. no.	Catchment	Observed climate	NCEP	NCEP_BC	ERA	ERA_BC
1.	Baitarani	8.2	14.7	12.3	11.3	11.2
2.	Ilmenau	1.7	2.9	2.4	2.6	2.4
3.	Itata	39.4	30.9	33.4	33	34.4
4.	Thubon	6.76	5.63	6.39	5.73	6.02

4.6. Optimization of available water resources

Table 10 shows the percentage change in the annual average irrigation and yield during deficit irrigation (Scenario: S2) compared to the optimal scenario (Scenario: S1) for all catchments. Only soil water deficit scenarios were used for this analysis, as they were providing more reliable irrigation water amounts as compared to the plant water stress scheduling. It can be seen from the table that the amount of irrigation applied during deficit irrigation is 25–48% less than the optimal irrigation, whereas the overall reduction in average crop yield varies from 0 to 3.3%. For the Ilmenau catchment, the findings are in a similar range as field experiments carried out by the local agricultural chamber in Hamerstorf, which showed irrigation water savings of 47% by deficit irrigation for winter wheat by a negligible change in yield for winter wheat, whereas for sugar beet 29% of water can be saved on the cost of 6% of yield (Fricke and Riedel, 2016). Therefore, it is clear from all the models that one can use deficit irrigation with small losses in the overall yield. This could be a good adaptation measure in concern of future water scarcity.

5. Conclusions

This study evaluated the application of SWAT in simulating irrigation water requirement in four different catchments around the globe (Chile, Germany, India and Vietnam). Modelling results revealed that the SWAT calibration was possible in four meso-scale catchments with good model efficiency (low bias) for streamflow with low percentage deviation in actual evapotranspiration in all the cases. The automatic irrigation provided plausible results for soil water scheduling in all the catchments with optimal and deficit strategies even if there was no

Table 10
Change in annual average irrigation and yield during deficit irrigation compared to optimal irrigation.

Catchments	% change	Observed climate	NCEP	NCEP_BC	ERA	ERA_BC
Baitarani	Irrigation	−37.44	−31.82	−32.70	−33.72	−33.68
	Yield	**−0.06**	**−1.63**	**−0.99**	**−0.48**	**−1.71**
Ilmenau	Irrigation	−43.33	−37.35	−38.50	−39.92	−40.96
	Yield	**−1.22**	**−1.68**	**−2.35**	**−1.69**	**−1.95**
Itata	Irrigation	−30.22	−29.65	−31.47	−40.60	−36.63
	Yield	**−0.75**	**−1.86**	**−1.65**	**−2.27**	**−2.18**
Thubon	Irrigation	−40.36	−48.39	−42.34	−42.25	−42.24
	Yield	**−3.33**	**−0.83**	**−1.82**	**−2.77**	**0.00**

comparison with observed values on that scale. There are indications that irrigation shows systematic overestimation though as reported by other authors before. Plant stress scheduling shows significant underestimation of irrigation water requirement in all catchments. The relatively low irrigation values in case of the plant stress method might be explained by possible errors associated with plant water stress algorithms embedded in the leaf area based crop growth model used by the SWAT. It can be concluded from the results that SWAT's mechanism for irrigation scheduling can be further improved.

The climate variables form NCEP and ERA exhibit different behavior in a catchment. Bias corrected rainfall, temperature and solar radiation datasets are more close to their observed counterparts than the uncorrected datasets. It can be inferred from the performance evaluation of reanalysis data that streamflow and irrigation simulated by the model highly depend on input data. Reanalysis datasets were biased in all the four catchments, and in all cases raw reanalysis data led to serious bias in the estimated evapotranspiration and irrigation requirement. Results showed that rainfall is not always the governing variable in irrigation simulation. Therefore, it is worth to investigate and bias correct the other climate variables. In addition to this, uncertainty exists in the climate reanalysis data; although an attempt has been made to check it via quantile mapping, still there is an acceptable bias in the quantile corrected reanalysis data. It can be deduced that for any given hydrological model not only the input data but also the input data variability plays an important role for the simulation of irrigated catchments. Climate change and adaptation studies must take that into account. The results strongly support the application of bias corrections, even if they can be criticized from the meteorological community due to disturbance of the physical consistency of climate variables. However, the relative effects of deficit irrigation strategies on water use and crop yield could be simulated by all datasets.

This study confirms the application of SWAT for regional irrigation studies, which are of high importance for water resources management. With today's improved data availability and computing power, models like SWAT might fill a gap between field scale models as often used in agriculture and large scale models, whose results have been questioned in other studies due to their large bias when evaluated on smaller scales. In the light of climate change and higher water demand for food production, more attention should be put on to the simulated irrigation amount at regional and global scale. Upscaling a regional model, driven by corrected global reanalysis data, might provide a more accurate estimation of irrigation water requirement than the global models due to their over simplification. Therefore, further research is needed in this direction for improving the global and regional water management.

Acknowledgement

This paper is a part of research performed by the corresponding author under the PhD funding provided by Indian Council of Agricultural Research. The authors are grateful to Van Tam Nguyen, Prajna Kasargodu Anebagilu and Jannatul Fardous for providing technical support and for proof reading. Authors wanted to thank the Vietnam Academy of Water Resources (Land Use and Climate Change Interactions in Central Vietnam Project) for providing the necessary data. In addition, the authors acknowledge the free provision of data for German and Chilean catchments provided by the respective authorities. We acknowledge funding of the collaboration between the universities of Hannover and Concepcion by BMBF grant 01DN13016.

References

Abbaspour, K.C., Rouholahnejad, E., Vaghefi, S., Srinivasan, R., Yang, H., Kløve, B., 2015. A continental-scale hydrology and water quality model for Europe: calibration and uncertainty of a high-resolution large-scale SWAT model. J. Hydrol. 524, 733–752.

Abrahamsen, P., Hansen, S., 2000. Daisy: an open soil-crop-atmosphere system model. Environ. Model. Softw. 15, 313–330.

Alemayehu, T., Griensven, A.V., Woldegiorgis, B.T., Bauwens, W., 2017. An improved SWAT vegetation growth module and its evaluation for four tropical ecosystems. Hydrol. Earth Syst. Sci. 21 (9), 4449–4467.

Allen, R.G., Perevia, L.S., Raes, D., Smith, M., 1998. Crop evapotranspiration: guidelines for computing crop water requirements. FAO Irrigation and Drainage Paper No. 56. Food and Agriculture Organization, Rome, Italy.

Allen, R., Irmak, A., Trezza, R., Hendrickx, J.M., Bastiaanssen, W., Kjaersgaard, J., 2011. Satellite-based ET estimation in agriculture using SEBAL and METRIC. Hydrol. Process. 25 (26), 4011–4027.

Arnold, J.G., Srinivasan, R., Muttiah, R.S., Williams, J.R., 1998. Large area hydrologic modeling and assessment part I: model development. J. Am. Water Resour. Assoc. 34 (1), 73–89.

Arnold, J.G., Bieger, K., White, M.J., Srinivasan, R., Dunbar, J.A., Allen, P.M., 2018. Use of decision tables to simulate management in SWAT+. Water 10 (6), 713.

Barr, A.G., Kite, G.W., Granger, R., Smith, C., 1997. Evaluating three evapotranspiration methods in the SLURP macroscale hydrological model. Hydrol. Process. 11 (13), 1685–1705.

Bastiaanssen, W.G.M., Menenti, M., Feddes, R.A., Holtslag, A.A.M., 1998. A remote sensing surface energy balance algorithm for land (SEBAL). 1. Formulation. J. Hydrol. 212, 198–212.

Bastiaanssen, W.G., Molden, D.J., Makin, I.W., 2000. Remote sensing for irrigated agriculture: examples from research and possible applications. Agric. Water Manag. 46 (2), 137–155.

Bastola, S., Misra, V., 2013. Evaluation of dynamically downscaled reanalysis precipitation data for hydrological application. Hydrol. Process. https://doi.org/10.1002/hyp.9734.

World agriculture: towards 2015/2030: an FAO perspective. In: Bruinsma, J. (Ed.), Earth Scan.

Chen, Y., Marek, G.W., Marek, T.H., Brauer, D.K., Srinivasan, R., 2017. Assessing the efficacy of the SWAT auto-irrigation function to simulate irrigation, evapotranspiration, and crop response to management strategies of the Texas High Plains. Water 9, 509.

Chen, Y., Marek, G.W., Marek, T.H., Brauer, D.K., Srinivasan, R., 2018. Improving SWAT auto-irrigation functions for simulating agricultural irrigation management using long-term lysimeter field data. Environ. Model. Softw. 99, 25–38.

Christensen, J.H., Boberg, F., Christensen, O.B., Lucas-Picher, P., 2008. On the need for bias correction of regional climate change projections of temperature and precipitation. Geophys. Res. Lett. 35 (20), 1–6.

Conrad, C., Colditz, R.R., Dech, S., Klein, D., Vlek, P.L., 2011. Temporal segmentation of MODIS time series for improving crop classification in central Asian irrigation systems. Int. J. Remote Sens. 32 (23), 8763–8778.

Cuenca, R.H., Ciotti, S.P., Hagimoto, Y., 2013. Application of Landsat to evaluate effects of irrigation forbearance. Remote Sens. 5 (8), 3776–3802.

Danner, C.L., 2006. Documentation and Testing of the WEAP Model for the Rio Grande/Bravo Basin. Texas University at Austin.

Dechmi, F., Burguete, J., Skhiri, A., 2012. SWAT application in intensive irrigation systems: model modification, calibration and validation. J. Hydrol. 470, 227–238.

Dee, D.P., Uppala, S.M., Simmons, A.J., Berrisford, P., Poli, P., Kobayashi, S., ... Bechtold, P., 2011. The ERA-interim reanalysis: configuration and performance of the data assimilation system. Q. J. R. Meteorol. Soc. 137 (656), 553–597.

Doorenbos, J., Pruitt, W.O., 1977. Guidelines for predicting crop water requirements. Irrigation and Drainage Paper No. 24. Rome, Italy. United Nations FAO.

Droogers, P., Bastiaanssen, W., 2002. Irrigation performance using hydrological and remote sensing modeling. J. Irrig. Drain. Eng. 128 (1), 11–18.

Dubey, S.K., Sharma, D., 2018. Assessment of climate change impact of yield of major crops in the Banas river basin, India. Sci. Total Environ. 635, 10–19.

Emam, A.F., Kappas, M., Linh, N.H.K., Renchin, T., 2017. Hydrological modeling and runoff mitigation in an ungauged basin of central Vietnam using SWAT model. Hydrology 4 (16), 1–17.

Essou, G.R., Arsenault, R., Brissette, F.P., 2016. Comparison of climate datasets for lumped hydrological modeling over the continental United States. J. Hydrol. 537, 334–345.

Essou, G.R., Brissette, F., Lucas-Picher, P., 2017. Impacts of combining reanalyses and weather station data on the accuracy of discharge modelling. J. Hydrol. 545, 120–131.

Esteve, P., Varela-Ortega, C., Blanco-Gutiérrez, I., Downing, T.E., 2015. A hydro-economic model for the assessment of climate change impacts and adaptation in irrigated agriculture. Ecol. Econ. 120, 49–58.

Firoz, A.B.M., Nauditt, A., Fink, M., Ribbe, L., 2018. Quantifying human impacts on hydrological drought using a combined modelling approach in a tropical river basin in central Vietnam. Hydrol. Earth Syst. Sci. 22 (1), 547–565.

Fricke, E., Riedel, A., 2016. Versuchsbericht 2016. Fachverband Feldbewässerung, Uelzen.

Gharbia, S.S., Smullen, T., Gill, L., Johnston, P., Pilla, F., 2018. Spatially distributed potential evapotranspiration modelling and climate projections. Sci. Total Environ. 633, 571–592.

Glenn, E.P., Doody, T.M., Guerschman, J.P., Huete, A.R., King, E.A., McVicar, T.R., van Dijk, J.M., van Neil, T.G., Yebra, M., Zhang, Y., 2011. Actual evapotranspiration estimation by ground and remote sensing methods: the Australian experience. Hydrol. Process. 25, 4103–4116.

Gupta, H.V., Kling, H., Yilmaz, K.K., Martinez, G.F., 2009. Decomposition of the mean squared error and NSE performance criteria: implications for improving hydrological modelling. J. Hydrol. 377 (1–2), 80–91.

Hai, L.T., 2003. The Organization of the Liberalized Rice Market in Vietnam (Doctoral Dissertation, Thesis for Award of PhD Degree at University Of Groningen, Groningen, Netherlands, 236pp).

Hwang, S., Graham, W.D., Geurink, J.S., Adams, A., 2014. Hydrologic implications of errors in bias-corrected regional reanalysis data for west central Florida. J. Hydrol. 510, 513–529.

Jiang, Y., Xu, X., Huang, Q., Huo, Z., Huang, G., 2015. Assessment of irrigation performance and water productivity in irrigated areas of the middle Heihe River basin using a distributed agro-hydrological model. Agric. Water Manag. 147, 67–81.

Kim, N.W., Lee, J., 2010. Enhancement of the channel routing module in SWAT. Hydrol. Process. 24 (1), 96–107.

Kite, G.W., 1998. Manual for the SLURP Hydrological Model. NHRI, Saskatoon, Canada.

Kite, G.W., Droogers, P., 2000. Comparing evapotranspiration estimates from satellites, hydrological models and field data. J. Hydrol. 229 (1–2), 3–18.

López, P.L., Sutanudjaja, E.H., Schellekens, J., Sterk, G., Bierkens, M., 2017. Calibration of a large-scale hydrological model using satellite-based soil moisture and evapotranspiration products. Hydrol. Earth Syst. Sci. 21, 3125–3144.

Loukas, A., Vasiliades, L., 2014. Streamflow simulation methods for ungauged and poorly gauged watersheds. Nat. Hazards Earth Syst. Sci. 14 (7), 1641.

Ma, Y., Feng, S., Huo, Z., Song, X., 2011. Application of the SWAP model to simulate the field water cycle under deficit irrigation in Beijing, China. Math. Comput. Model. 54 (3–4), 1044–1052.

Maier, N., Dietrich, J., 2016. Using SWAT for strategic planning of basin scale irrigation control policies: a case study from a humid region in northern Germany. Water Resour. Manag. 30 (9), 3285–3298.

Marek, G.W., Gowda, P.H., Evett, S.R., Baumhardt, R.L., Brauer, D.K., Howell, T.A., Marek, T.H., Srinivasan, R., 2016. Estimating evapotranspiration for dryland cropping systems in the semiarid Texas high plains using SWAT. J. Am. Water Resour. Assoc. 52 (2), 298–314.

Mehta, V.K., Haden, V.R., Joyce, B.A., Purkey, D.R., Jackson, L.E., 2013. Irrigation demand and supply, given projections of climate and land-use change, in Yolo County, California. Agric. Water Manag. 117, 70–82.

Meinardus, A., Griggs, R.H., Benson, V., Williams, J., 1998. EPIC. Temple. Blackland Research and Extension Center, Texas www.brc.tamus.edu/epic, Accessed date: 21 January 2016.

Moriasi, D.N., Arnold, J.G., Van Liew, M.W., Bingner, R.L., Harmel, R.D., Veith, T.L., 2007. Model evaluation guidelines for systematic quantification of accuracy inwatershed simulations. Trans. ASABE 50 (3), 885–900.

Mu, Q., Zhao, M., Running, S.W., 2013. MODIS global terrestrial evapotranspiration (ET) product (NASA MOD16A2/A3). Algorithm Theoretical Basis Document, Collection. 5.

Muñoz, E., Arumí, J.L., Wagener, T., Oyarzún, R., Parra, V., 2016. Unraveling complex hydrogeological processes in Andean basins in south-central Chile: an integrated assessment to understand hydrological dissimilarity. Hydrol. Process. 30 (26), 4934–4943.

Nam, D.H., Udo, K., Mano, A., 2013. Assessment of future flood intensification in Central Vietnam using a super-high-resolution climate model output. J. Water Clim. Chang. 4 (4), 373–389.

Nayak, A.B., 2006. An Analysis Using Liss III Data for Estimating Water Demand for Rice Cropping in Parts of Hirakud Command Area. ITC, Orissa, India.

Nay-Htoon, B., Phong, N.T., Schlüter, S., Janaiah, A., 2013. A water productive and economically profitable paddy rice production method to adapt water scarcity in the Vu Gia-Thu Bon river basin, Vietnam. J. Nat. Resour. Dev. 3, 58–65.

Neitsch, S.L., Arnold, J.G., Kiniry, J.R., Williams, J.R., 2011. Soil and Water Assessment Tool Theoretical Documentation Version 2009. Texas Water Resources Institute.

Niehoff, D., Fritsch, U., Bronstert, A., 2002. Land-use impacts on storm-runoff generation: scenarios of land-use change and simulation of hydrological response in a meso-scale catchment in SW-Germany. J. Hydrol. 267 (1–2), 80–93.

Ozdogan, M., Yang, Y., Allez, G., Cervantes, C., 2010. Remote sensing of irrigated agriculture: opportunities and challenges. Remote Sens. 2 (9), 2274–2304.

Panagopoulos, Y., Makropoulos, C., Gkiokas, A., Kossida, M., Evangelou, L., Lourmas, G., Michas, S., Tsadilas, C., Papagerorgiou, S., Perleros, V., Darkopoulou, S., Mimikou, M., 2014. Assessing the cost-effectiveness of irrigation water management practices in water stressed agricultural catchments: the case of Pinios. Agric. Water Manag. 139, 31–42.

Peel, M.C., Finlayson, B.L., McMahon, T.A., 2007. Updated world map of the Köppen-Geiger climate classification. Hydrol. Earth Syst. Sci. Discuss. 4 (2), 439–473.

Peña-Arancibia, J.L., Mainuddin, M., Kirby, J.M., Chiew, F.H., McVicar, T.R., Vaze, J., 2016. Assessing irrigated agriculture's surface water and groundwater consumption by combining satellite remote sensing and hydrologic modelling. Sci. Total Environ. 542, 372–382.

Pervez, M.S., Brown, J.F., 2010. Mapping irrigated lands at 250-m scale by merging MODIS data and national agricultural statistics. Remote Sens. 2 (10), 2388–2412.

Piani, C., Haerter, J.O., Coppola, E., 2010a. Statistical bias correction for daily precipitation in regional climate models over Europe. Theor. Appl. Climatol. 99 (1–2), 187–192.

Piani, C., Weedon, G.P., Best, M., Gomes, S.M., Viterbo, P., Hagemann, S., Haerter, J.O., 2010b. Statistical bias correction of global simulated daily precipitation and temperature for the application of hydrological models. J. Hydrol. 395 (3–4), 199–215.

Plesca, I., Timbe, E., Exbrayat, J.-F., Windhorst, D., Kraft, P., Crespo, P., Vache, K.B., Frede, H.-G., Breuer, L., 2012. Model intercomparison to explore catchment functioning: results from a remote montane tropical rainforest. Ecol. Model. 239, 3–13.

Polanco, E.I., Fleifle, A., Ludwig, R., Disse, M., 2017. Improving SWAT model performance in the upper Blue Nile Basin using meteorological data integration and subcatchment discretization. Hydrol. Earth Syst. Sci. 21 (9), 4907–4926.

Poveda, G., Waylen, P.R., Pulwarty, R.S., 2006. Annual and inter-annual variability of the present climate in northern South America and southern Mesoamerica. Palaeogeogr. Palaeoclimatol. Palaeoecol. 234 (1), 3–27.

Rabie, Z., Honar, T., Kazemi, A.R., 2013. Optimal, simultaneous land and water allocation under resource limitation conditions, using soil water balance (case study of Doroudzan dam irrigation and drainage network). J. Irrig. Drain. Eng. 2 (7), 159–166.

Rockström, J., Falkenmark, M., 2000. Semiarid crop production from a hydrological perspective: gap between potential and actual yields. Crit. Rev. Plant Sci. 19 (4), 319–346.

Romaguera, M., Krol, M.S., Salama, M., Hoekstra, A.Y., Su, Z., 2012. Determining irrigated areas and quantifying blue water use in Europe using remote sensing Meteosat second generation (MSG) products and global land data assimilation system (GLDAS) data. Photogramm. Eng. Remote. Sens. 78 (8), 861–873.

Saha, S., Moorthi, S., Pan, H.L., Wu, X., Wang, J., Nadiga, S., ... Liu, H., 2010. The NCEP climate forecast system reanalysis. Bull. Amer. Meteor. Soc. 91 (8), 1015–1058.

Santhi, C., Muttiah, R.S., Arnold, J.G., Srinivasan, R., 2005. A GIS-based regional planning tool for irrigation demand assessment and savings using SWAT. Am. Soc. Agric. Eng. 48 (1), 137–147.

Scanlon, B., Jolly, I., Sophocleous, M., Zhang, L., 2007. Global impacts of conversions from natural to agricultural ecosystems on water resources: quantity versus quality. Water Resour. Res. 43 (3), W03437.

Schulla, J., Jasper, K., 2007. Model Description Wasim-eth. Institute for Atmospheric and Climate Science, Swiss Federal Institute of Technology, Zürich.

Searcy, J.K., Hardison, C.H., 1960. Double-mass curves. Manual of Hydrology: Part 1. General Surface-water Techniques. Geological Survey Water-Supply Paper 1541-B.

Shrestha, S., Deb, P., Bui, T.T.T., 2016. Adaptation strategies for rice cultivation under climate change in Central Vietnam. Mitig. Adapt. Strateg. Glob. Chang. 21 (1), 15–37.

Siebert, S., Döll, P., Hoogeveen, J., Faures, J.M., Frenken, K., Feick, S., 2005. Development and validation of the global map of irrigation areas. Hydrol. Earth Syst. Sci. Discuss. 2 (4), 1299–1327.

Singh, R., Kroes, J.G., van Dam, J.C., Feddes, R.A., 2006. Distributed ecohydrological modelling to evaluate the performance of irrigation system in Sirsa district, India: I. Current water management and its productivity. J. Hydrol. 329 (3–4), 692–713.

Sivapalan, M., Takeuchi, K., Franks, S.W., Gupta, V.K., Karambiri, H., Lakshmi, V., Liang, X., McDonnell, J.J., Mendiondo, E.M., O'Connell, P.E., Oki, T., Pomeroy, J.W., Schertzer, D., Uhlenbrook, S., Zehe, E., 2003. IAHS decade on predictions in ungauged basins (PUB), 2003–2012: shaping an exciting future for the hydrological sciences. Hydrol. Sci. J. 48 (6), 857–880.

Stammerjohn, S.E., Martinson, D.G., Smith, R.C., Iannuzzi, R.A., 2008. Sea ice in the western Antarctic Peninsula region: Spatio-temporal variability from ecological and climate change perspectives. Deep-Sea Res. II Top. Stud. Oceanogr. 55 (18), 2041–2058.

Steele, D.D., Thoreson, B.P., Hopkins, D.G., Clark, B.A., Tuscherer, S.R., Gautam, R., 2015. Spatial mapping of evapotranspiration over Devils Lake basin with SEBAL: application to flood mitigation via irrigation of agricultural crops. Irrig. Sci. 33 (1), 15–29.

Stehr, A., Debels, P., Arumi, J.L., Romero, F., Alcayaga, H., 2009. Combining the Soil and Water Assessment Tool (SWAT) and MODIS imagery to estimate monthly flows in a data-scarce Chilean Andean basin. Hydrol. Sci. J. 54 (6), 1053–1067.

Tang, Q., Peterson, S., Cuenca, R.H., Hagimoto, Y., Lettenmaier, D.P., 2009a. Satellite-based near-real-time estimation of irrigated crop water consumption. J. Geophys. Res.-Atmos. 114 (D5), 1–14.

Tang, Q., Rosenberg, E.A., Lettenmaier, D.P., 2009b. Use of satellite data to assess the impacts of irrigation withdrawals on Upper Klamath Lake, Oregon. Hydrol. Earth Syst. Sci. 13 (5), 617–627.

Teixeira, A.D.C., Bastiaanssen, W.G.M., Ahmad, M.U.D., Bos, M.G., 2009. Reviewing SEBAL input parameters for assessing evapotranspiration and water productivity for the low-middle Sao Francisco River basin, Brazil: part A: calibration and validation. Agric. For. Meteorol. 149 (3–4), 462–476.

Teutschbein, C., Seibert, J., 2010. Regional climate models for hydrological impact studies at the catchment scale: a review of recent modeling strategies. Geogr. Compass 4 (7), 834–860.

Thenkabail, P.S., Biradar, C.M., Noojipady, P., Dheeravath, V., Li, Y., Velpuri, M., Gumma, M., Gangalakunta, O.R.P., Turral, H., Cai, X., Vithanage, J., 2009. Global irrigated area map (GIAM), derived from remote sensing, for the end of the last millennium. Int. J. Remote Sens. 30 (14), 3679–3733.

Thrasher, B., Maurer, E.P., McKellar, C., Duffy, P.B., 2012. Bias correcting climate model simulated daily temperature extremes with quantile mapping. Hydrol. Earth Syst. Sci. 16 (9), 3309–3314.

Udias, A., Pastori, M., Malango, A., Vigiak, O., Nikolaidias, N.P., Bouraoui, F., 2018. Identifying efficient agricultural irrigation strategies in Crete. Sci. Total Environ. 633, 271–284.

Uniyal, B., Dietrich, J., Vasilakos, C., Tzoraki, O., 2017. Evaluation of SWAT simulated soil moisture at catchment scale byfield measurements and Landsat derived indices. Agric. Water Manag. 193, 55–70.

Ut, T.T., Kajisa, K., 2006. The impact of green revolution on rice production in Vietnam. Dev. Econ. 44 (2), 167–189.

van Dam, J.C., Huygen, J., Wesseling, J.G., Feddes, R.A., Kabat, P., van Walsum, P.E.V., ... van Diepen, C.A., 1997. Theory of SWAP Version 2.0; Simulation of Water Flow, Solute Transport and Plant Growth in the Soil-water-atmosphere-plant Environment (No. 71, p. 167). DLO Win and Staring Centre.

van Griensven, A., Ndomba, P., Yalew, S., Kilonzo, F., 2012. Critical review of SWAT applications in the upper Nile basin countries. Hydrol. Earth Syst. Sci. 16, 3371–3381.

van Niel, T.G., McVicar, T.R., 2004. Current and potential uses of optical remote sensing in rice-based irrigation systems: a review. Aust. J. Agric. Res. 55 (2), 155–185.

Varis, O., Kajander, T., Lemmelä, R., 2004. Climate and water: from climate models to water resources management and vice versa. Clim. Chang. 66 (3), 321–344.

Verma, A.K., Jha, M.K., 2015. Evaluation of a GIS-based watershed model for streamflow and sediment-yield simulation in the upper Baitarani river basin of Eastern India. J. Hydrol. Eng. 20 (6), C5015001–C5015012.

Vervoort, R.W., Miechels, S.F., van Ogtrop, F.F., Guillaume, J.H., 2014. Remotely sensed evapotranspiration to calibrate a lumped conceptual model: pitfalls and opportunities. J. Hydrol. 519, 3223–3236.

Vidal, I., Longeri, L., Hétier, J.M., 1999. Nitrogen uptake and chlorophyll meter measurements in spring wheat. Nutr. Cycl. Agroecosyst. 55 (1), 1–6.

Walker, W.R., Prajamwong, S., Allen, R.G., Merkley, G.P., 1995. USU command area decision support model—CADSM. Crop-water-simulation Models in Practice. Wageningen Pers, Wageningen, pp. 231–271.

Wang, X.L., Swail, V.R., Zwiers, F.W., 2006. Climatology and changes of extratropical cyclone activity: comparison of ERA-40 with NCEP–NCAR reanalysis for 1958–2001. J. Clim. 19 (13), 3145–3166.
Wang, Y., Chen, Y., Peng, S., 2011. A GIS framework for changing cropping pattern under different climate conditions and irrigation availability scenarios. Water Resour. Manag. 25 (13), 3073–3090.
Williams, J.R., Jones, C.A., Kiniry, J., Spanel, D.A., 1989. The EPIC crop growth model. Trans. ASAE 32 (2), 497–511.
Wisser, D., Frolking, S., Douglas, E.M., Fekete, B.M., Vörösmarty, C.J., Schumann, A.H., 2008. Global irrigation water demand: variability and uncertainties arising from agricultural and climate data sets. Geophys. Res. Lett. 35 (24), 1–5.
Wittenberg, H., 2003. Effects of season and man-made changes on baseflow and flow recession: case studies. Hydrol. Process. 17 (11), 2113–2123.
Wittenberg, H., 2015. Groundwater abstraction for irrigation and its impacts on low flows in a watershed in Northwest Germany. Resources 4 (3), 566–576.
Xie, X., Cui, Y., 2011. Development and test of SWAT for modeling hydrological processes in irrigation districts with paddy rice. J. Hydrol. 396 (1), 61–71.
Zhang, Y., Chiew, F.H., Zhang, L., Li, H., 2009. Use of remotely sensed actual evapotranspiration to improve rainfall–runoff modeling in Southeast Australia. J. Hydrometeorol. 10 (4), 969–980.
Zhang, C., Liu, J., Shang, J., Cai, H., 2018. Capability of crop water content for revealing variability of winter wheat grain yield and soil moisture under limited irrigation. Sci. Total Environ. 631-632, 677–687.
Zuo, D., Xu, Z., Peng, D., Song, J., Cheng, L., Wei, S., Abbaspour, K.C., Yang, H., 2015. Simulating spatiotemporal variability of blue and green water resources availability with uncertainty analysis. Hydrol. Process. 29 (8), 1942–1955.
Zwart, S.J., Bastiaanssen, W.G., 2007. SEBAL for detecting spatial variation of water productivity and scope for improvement in eight irrigated wheat systems. Agric. Water Manag. 89 (3), 287–296.